

April 16, 2013

The Reviewers,  
IEEE Transaction on Geoscience and Remote Sensing

Dear Reviewers,

We appreciate your time and effort in reviewing this paper. We hope that, like us when we were faced with its results, you will find satisfaction as well as excitement after reading through this paper. We appreciate your feedback in whatever way it may be in making this manuscript to become a better publication. To facilitate your review, we enclose here a short synopsis of the paper.

We are aware that the paper is a bit too long. Specifically, the mathematical derivations in the Appendices is presented in great details. While this is supposed to expediate your review, it probably should be shortened in publication. We would appreciate it if you can help us in pointing out which portion of this can be removed.

Once again, thank you for your reviewing time and effort.

Our best regards

The Authors

encl: The Synposis of the Paper: next page

**The Research Context:**

The extension from SAR to POLSAR brings about the representation issue in that: there exists not one, like the intensity in SAR, but many observable quantities in POLSAR.

**Problem Statement:**

While different statistical models have been developed for different POLSAR observables, for a model to be useful, discrimination measures need to be derived. Many POLSAR data processing techniques requires a scalar, representative observable and statistical model. Practical application for POLSAR data processing requires the measures to be scalar, consistent and preferably homoskedastic on one hand. On the other hand, the observable quantity being modelled need to be naturally representative for the high-dimensional POLSAR data.

**Claimed Solution:**

In this paper, a few statistical models for the determinant of the POLSAR covariance matrix are proposed. The models are believed to be representative since the determinant is transformed into the representative intensity when the multi-dimensional POLSAR data is collapsed into the one-dimensional case of traditional SAR data.

**Shortcomings of the current POLSAR statistical models:**

There are a few statistical models for POLSAR, but none of them result in a scalar discrimination measures. There are also a few POLSAR discrimination measures, but all of them are based on the likelihood test statistics, which regrettably only based on asymptotic distribution.

**Contributions of this paper**

This paper proposes a few statistical models for the determinant of POLSAR covariance matrix, which is shown to be the representative observable for the complex POLSAR data-set in the sense that this observable is the generalized version of the representative SAR intensity in the multi-dimensional case. Compared with other statistical models for POLSAR, the proposed models are scalar, and representative for POLSAR data. Moreover, several multiplicative dis-similarity measures and additive measures of distance are derived from the proposed statistical models. Compared with other discrimination measure proposals, this paper suggests an exact distribution for the POLSAR likelihood statistical test. As a by-product of this exact modelling, a simpler measure of distance, i.e. contrast, is proposed for the common case of  $Lx = Ly$ .

# Scalar and Representative Models for Polarimetric SAR Data

Thanh-Hai Le, Ian McLoughlin, and Chan-Hua Vun

## Abstract

While statistical models are important in understanding the stochastic nature of Polarimetric SAR (POLSAR), scalar discrimination measures are routinely used in processing this multi-dimensional data. Ideally speaking, the latter should be driven from the former. As far as we know, however, it has not exactly been so for the case of POLSAR. In this paper, a couple of statistical models for the determinant of the POLSAR covariance matrix and its log-transformed derivations are proposed. These scalar models for the determinant of the POLSAR covariance matrix are shown to be representative since this observable is neatly transformed into the traditional SAR intensity when the generic multi-dimensional polarimetry is collapsed into the case of one-dimensional SAR. Similar to SAR, the generic model for POLSAR is also shown to be multiplicative and heteroskedastic in the original domain and the logarithmic transformation converts this into a more familiar additive and homoskedastic model. Moreover, the scalar property of these statistical models lead to the derivation of several statistical discrimination measures. All of these statistical models are validated on real-life captured data and they are shown to be applicable even when the theoretical “independent samples” assumption is violated in practice. The combination of scalar, additive and homoskedastic properties of the derived statistical models bring about a couple of benefits, which are also described in this paper. First, compared to the original multiplicative domain, the additive log-transformed fit more naturally with the linear nature of digital imagery. Second, since the Gauss-Markov theorem is again applicable in the homoskedastic log-transformed domain, the use of Mean Squared Error (MSE) as an reliable objective function for POLSAR speckle filters is briefly explored.

## Index Terms

Thanh-Hai Le and Chan-Hua Vun are with School of Computer Engineering, Nanyang Technological University, Singapore. Ian McLoughlin is with School of Information Science and Technology, University of Science and Technology of China.

Manuscript received ?, 2013; revised ?.

Polarimetric Synthetic aperture radar, Electromagnetic Modeling, Multidimensional signal processing

## I. INTRODUCTION

In the past decades, the exponential growth in computational power has made the once overly-excessive computationally-demanding SAR technology now become a feasible and preferred earth observation solution. As state-of-the-art technology, the SAR technique has been extended in a few directions, one of which is the polarimetric SAR or POLSAR. POLSAR is the natural extension from SAR exploiting the natural polarization property of Electro-Magnetic (EM) waves. Similar to the extension from black-and-white images to color photography, the polarimetric extension brought about the multi-channels POLSAR data as compared to the traditional one-channel SAR data.

With (POL)SAR data becomes cheaper and more available, the recent research emphasis is on understanding and developing applications for the data. The complex data, however is stochastic by nature, due to the interference phenomena of EM waves. Under this condition, it is very important to understand the statistical models for (POL)SAR data.

While the statistical models for homogeneous areas of one-dimensional SAR data have been developed, in extending our understanding towards multi-dimensional POLSAR data, an important issue needs to be addressed. The trouble that the high dimensional data bring about is that there exists not one, as the intensity in the one-channel SAR, but many observables quantities in multi-channel POLSAR. While different statistical models have been developed for different POLSAR observables, for a statistical model to be useful, scalar discrimination measures need to be derived from it. Thus practical application for POLSAR data processing requires the dissimilarity measure to be scalar, consistent and preferably homoskedastic on one hand. On the other hand, the observable quantity being modelled needs to be naturally representative for the high dimensional POLSAR data.

In this paper, the determinant of the POLSAR covariance matrix is proposed as an observable quantity to study. The representative power of this observable is demonstrated when the multi-dimensional POLSAR data is collapsed into the traditional one-dimensional SAR scenario. Under this transformation, the determinant of the POLSAR covariance matrix is converted into the standard SAR intensity. Statistical models for this heteroskedastic POLSAR determinant and

homoskedastic log-determinant are then derived. And since POLSAR can be viewed as a multi-dimensional extension of SAR, the paper describes how the standard statistical models for SAR can be put within the natural coverage of this generic models for POLSAR.

Specifically, the rest of this paper is structured as follows. After the related work in literature is critically reviewed in Section II, Section III presents the theoretical models for both partial and full polarimetric SAR and their derived discrimination measures. The representative power of the scalar models are illuminated in Section IV, which details how the proposed models for the multi-variate POLSAR also includes the well-known models for the traditional SAR as its special univariate case. Besides being theoretically comprehensive, the model is also shown, in Section V, to be robust in handling practical data. To demonstrate the application of these scalar and representative models, Section VI explores how they can be used to evaluate POLSAR speckle filters. In the end, Section VII provides the final conclusion of the paper.

## II. RELATED WORK IN LITERATURE

This section critically review the related work in published literature. Specifically, the first sub-section shows that while many discrimination measures have been proposed for POLSAR data, almost all of them depends on the likelihood statistical test for complex Wishart distribution. Unfortunately, in the original proposed work [1], while an exact distribution is to be expected, only an asymptotic distribution was given. The second sub-section reviews various statistical models for different POLSAR observables. Its purpose is to show that none of these models, as far as we know, led to statistically consistent discrimination measures.

### A. *POLSAR Discrimination Measures*

This sub-section reviews some relevant and published works relating to different measures of distance for POLSAR data. In particular, a few different matrix distances have been proposed and evaluated in recent review papers [2] [3] will be briefly reviewed.

The commonly used measure of distance for matrices are either the Euclidean or the Manhattan

distance, which are defined in the following equations, respectively:

$$d(C_x, C_y) = \sum_{i,j} |\Re(C_x - C_y)_{i,j}| + \sum_{i,j} |\Im(C_x - C_y)_{i,j}| \quad (1)$$

$$d(C_x, C_y) = \sqrt{\sum_{i,j} |C_x - C_y|_{i,j}^2} \quad (2)$$

where  $A_{i,j}$  denotes the (i,j) elements of the matrix A,  $||$  denotes absolute values and  $\Re, \Im$  denote the real and imaginary parts respectively. However, in the context of POLSAR covariance matrix, these dis-similarity measures are not widely used probably because of the multiplicative nature of the data.

In the field of POLSAR, the Wishart Distance is probably the most widely used as part of the well-known Wishart Classifier [4]. The distance is defined as [5]

$$d(C_x, C_y) = \ln |C_y| + \text{tr}(C_x C_y^{-1}) \quad (3)$$

As a measure of distance, its main disadvantage is that  $d(C_y, C_y) = \ln |C_y| \neq 0$ .

Recent works have suggested a number of other dissimilarity measures. These include the asymmetric and symmetric refined wishart distance [6],

$$d(C_x, C_y) = \frac{1}{2} \text{tr}(C_x^{-1} C_y + C_y^{-1} C_x) - d \quad (4)$$

$$d(C_x, C_y) = \ln |C_x| - \ln |C_y| + \text{tr}(C_x C_y^{-1}) - d \quad (5)$$

the Bartlett distance [3],

$$d(C_x, C_y) = 2 \ln |C_{x+y}| - \ln |C_x| - \ln |C_y| - 2d \ln 2 \quad (6)$$

the Bhattacharyya distance [7],

$$r(C_x, C_y) = \frac{|C_x|^{1/2} |C_y|^{1/2}}{|(C_x + C_y)/2|} \quad (7)$$

and the Wishart Statistical test distance [8]

$$d(C_x, C_y) = (L_x + L_y) \ln |C| - L_x \ln |C_x| - L_y \ln |C_y| \quad (8)$$

.

In comparison to these formulae, the distance measures for two covariance matrices proposed in this paper can be written as:

$$d(C_x, C_y) = \ln |C_x| - \ln |C_y| \quad (9)$$

At first glance, while the propose formula may be a lot simpler, it still operates in a similar way to others in making use of the log-determinant.

Closer investigation of these dis-similarity measures reveals that most of them are related to each other. The Bhattacharyya distance is easily shown to be related to the Barlett distance. At the same time the Barlett distance can be considered as the special case of the Wishart Statistical Test distance, where the two data set have the same number of look, i.e.  $L_x = L_y$ . It is also intuitively trivial to arrive at the conclusion that the contrast measure of distance proposed in this paper has fixed statistical behaviour, by comparing the symmetric and asymmetric versions of the refined Wishart distance, assuming that they are shown to follow fixed distributions.

The close relation among these is further supported by the fact that all of the papers proposing these measures referenced the statistical model developed in [1] as their foundation. In [1], to determine if the two scaled multi-look POLSAR covariance matrix  $Z_x$  and  $Z_y$ , which have  $L_x$  and  $L_y$  as the corresponding number of looks, come from the same underlying stochastic process, the likelihood ratio statistics for POLSAR covariance matrix is considered:

$$Q = \frac{(L_x + L_y)^{d(L_x + L_y)}}{L_x^{d \cdot L_x} L_y^{d \cdot L_y}} \frac{|Z_x|^{L_x} |Z_y|^{L_y}}{|Z_x + Z_y|^{(L_x + L_y)}}$$

Taking the log-transformation of the above statistics, and note that  $C_{vx} = Z_x/L_x$ ,  $C_{vy} = Z_y/L_y$  and  $C_{vxy} = (Z_x + Z_y)/(L_x + L_y)$  it becomes

$$Q = \frac{|C_{vx}|^{L_x} \cdot |C_{vy}|^{L_y}}{|C_{vxy}|^{L_x + L_y}} \quad (10)$$

$$\ln Q = L_x \ln |C_{vx}| + L_y \ln |C_{vy}| - (L_x + L_y) \ln |C_{vxy}| \quad (11)$$

To detect changes, a test statistics is developed based on this measure of distance. This means a distribution is to be derived for the dissimilarity measure. However, originally in the proposed work [1], only an asymptotic distribution is derived. Since both  $Z_x$  and  $Z_y$  follow a complex Wishart distribution with  $L_x$  and  $L_y$  degrees of freedom,  $Z_x + Z_y$  also follows the complex Wishart distribution with  $(L_x + L_y)$  degrees of freedom. In view of the models for  $|C_v|$  and  $\ln |C_v|$  developed in this paper (Eqns. 19 & 20), it is evident that not only the bound for  $\ln Q$ , or equivalently  $Q$ , can be derived but the whole statistical distribution for it can be simulated as well.

### B. Scalar Observables and Statistical Models for POLSAR Data

Of course, discrimination measures are not the only way to carry out classification tasks in POLSAR. Another common approach is to carry out classification using POLSAR observables identified by different target decomposition theorems. In [9], the performance of different scalar POLSAR observables for classification purposes is evaluated. While many scalar observables for POLSAR were presented, their corresponding statistical models and classifiers were not available. Furthermore, at its conclusion, the paper indicated that “it is impossible to identify the best one” as these “representations ... do not show a precise trend”. To be fair, these observables are identified to describe a decomposed portion of the complex POLSAR data, and thus they are not to be used individually for the purpose of single-handedly representing POLSAR data.

Given the joint distribution for POLSAR is known to be the multi-variate Complex Wishart distribution, it is possible to derive the scalar statistical models for some univariate POLSAR observables. However, such derivations are no trivial tasks, as the data is much more complex and the field is much less matured than the traditional SAR statistical modelling. Thus the strategy of the pioneering work is to tackle simpler versions of polarimetry.

POLSAR data is commonly represented by its covariance matrix. For full-pol the covariance matrix has the form of

$$C_3 = \begin{bmatrix} S_{hh}^2 & \sqrt{2}S_{hh}S_{hv}^* & S_{hh}S_{vv}^* \\ \sqrt{2}S_{hh}^*S_{hv} & 2S_{hv}^2 & \sqrt{2}S_{hv}S_{vv}^* \\ S_{hh}^*S_{vv} & \sqrt{2}S_{hv}^*S_{vv} & S_{vv}^2 \end{bmatrix}$$

For part-pol, it reduces to either:

$$C_{2,h} = \begin{bmatrix} S_{hh}^2 & S_{hh}S_{hv}^* \\ S_{hh}^*S_{hv} & S_{hv}^2 \end{bmatrix}; C_{2,v} = \begin{bmatrix} S_{hv}^2 & S_{hv}S_{vv}^* \\ S_{hv}^*S_{vv} & S_{vv}^2 \end{bmatrix}$$

Obviously, the statistical behavior of  $C_3$  can be understood by understanding the behavior of  $C_{2h}$ ,  $C_{2v}$  and

$$C_{2,c} = \begin{bmatrix} S_{hh}^2 & S_{hh}S_{vv}^* \\ S_{hh}^*S_{vv} & S_{vv}^2 \end{bmatrix}$$

While  $C_{2v}$ ,  $C_{2h}$  are physically related to the Stokes parameters of EM waves,  $C_{2c}$  is a totally made-up mathematical term from the full-pol covariance matrix. In fact, in the field of Polarimetric SAR,  $C_{2v}$ ,  $C_{2h}$  is called cross-pol and  $C_{2c}$  is called co-pol covariance matrices. Their



main difference lies in investigating the so-called complex correlation coefficient, defined as:

$$\rho = \frac{E(S_{pq}S_{rs}^*)}{\sqrt{E(S_{pq}^2)E(S_{rs}^2)}} = |\rho|e^{j\phi}$$

with  $\phi = \arg(\rho)$  is the phase difference angle. In  $C_{2v}, C_{2h}$  of optical physics,  $|\rho_v|, |\rho_h|$  are insignificant, and  $\phi_v, \phi_h$  are very random, due to little correlation between orthogonal polarization in monochromatic EM waves. Their equivalent lie in the “natural surface” case of POLSAR, where it is common to consider:  $|\rho_v| = |\rho_h| = 0$ . This is, however, not true in the general case of POLSAR. Specifically for  $C_{2c}$ , since there are correlation between the two co-pol channels,  $|\rho_c|$  is almost always significant and  $\phi_c$  is also not entirely random.

In the field of optical physics, under the assumption of no correlation between cross-polarized channels, [10], [11] and [12] derived the statistical models for  $C_{2h}, C_{2v}$ . The observables that have been studied are:

- 1) the polarization ellipse parameters [10]: i.e.
  - a) the total power  $S_0 = C_{11}^2 + C_{22}^2$ ,
  - b) the ratio of minor to major axis of the polarization ellipse  $\epsilon = \lambda_2/\lambda_1$ ,
  - c) and  $\psi$  the angle that the ellipse major axis makes with horizontal axis,
- 2) the Stokes parameters [11]: i.e.
  - a)  $S_0 = C_{11}^2 + C_{22}^2$
  - b)  $S_1 = C_{11}^2 - C_{22}^2$
  - c)  $S_2 = \Re(C_{12})$
  - d)  $S_3 = \Im(C_{12})$
- 3) and the normalized Stokes parameters  $s_i = S_i/S_0, i > 0$  [12]

In the field of POLSAR, under the assumption of significant correlation between polarized channels, [13], [14] and [15] derived the statistical models for note only  $C_{2h}, C_{2v}$  but also  $C_{2c}$ . Specifically the following observables were studied:

- 1) cross-pol ratio  $r_{HV/HH} = |S_{HV}|^2/|S_{HH}|^2$  [13],
- 2) co-pol ratio  $r_{VV/HH} = |S_{VV}|^2/|S_{HH}|^2$  [13],
- 3) co-pol phase difference  $\phi_{VV/HH} = \arg(S_{VV}S_{HH}^*)$  [13] [14],
- 4) magnitude  $g = |\text{avg}(S_{pq}S_{rs}^*)|$  [14],
- 5) normalized magnitude  $\xi = \frac{|\text{avg}(S_{pq}S_{rs}^*)|}{\sqrt{\text{avg}(|S_{pq}|^2)\text{avg}(|S_{rs}|^2)}}$  [14],

- 6) intensity ratio  $w = \text{avg}(|S_{pq}|^2)/\text{avg}(|S_{rs}|^2)$  [14],
- 7) and the Stokes parameters  $S_i, 0 \leq i \leq 3$  [15].

Furthermore, other studies has offered the statistical model for each element of the POLSAR covariance matrix  $S_{pq}S_{rs}^*$  [16] as well as the largest eigen-value of the covariance matrix  $\lambda_1$  [17]. While these models undoubtedly help in understanding the SAR data, individually none of them statisfies the dual criteria of 1) resulting in statistically consistent discrimination measures and 2) being an representative observable for the complex POLSAR data.

### III. THE SCALAR STATISTICAL MODELS FOR POLSAR

In this section, several scalar statistical models for POLSAR are presented. After the first sub-section briefly reviews related work in published literature, sub-section III-B presents the theoretical models together with conclusive evidence for two related points. The first point is that: POLSAR data is multiplicative and heteroskedastic in its original domain. And the second conclusion being: log-transformation converts it into an additive and homoskedastic model. Consequently a few consistent measures of distance are presented in section III-C.

#### A. The Basics of POLSAR Statistical Analysis

In this paper, the POLSAR scattering vector is denoted as  $s$ . In the case of partial polarimetric SAR (single polarization in transmit and dual polarization in receipt), the vector is two-dimensional ( $d = 2$ ) and is normally written as:

$$s_{part} = \begin{bmatrix} S_h \\ S_v \end{bmatrix} \quad (12)$$

In the case of full and monostatic POLSAR data, the vector is three-dimensional ( $d = 3$ ) and is presented as:

$$s_{full} = \begin{bmatrix} S_{hh} \\ \sqrt{2}S_{hv} \\ S_{vv} \end{bmatrix} \quad (13)$$

Let  $\Sigma = E[ss^{*T}]$  denote the population expected value of the POLSAR covariance matrix, where  $s^{*T}$  denotes the complex conjugate transpose of  $s$ . Assuming  $s$  is jointly circular complex

Gaussian with the expected covariance matrix  $\Sigma$ , then the probably density function (PDF) of  $s$  can be written as:

$$pdf(s; \Sigma) = \frac{1}{\pi^d |\Sigma|} e^{-s^{*T} \Sigma^{-1} s} \quad (14)$$

where  $||$  denotes the matrix determinant.

As the covariance matrix is only defined on multiple data points, sample POLSAR covariance matrices are commonly presented in “ensemble” format. They are formed as the mean of Hermitian outer product of single-look scattering vectors,

$$C_v = \langle s s^{*T} \rangle = \frac{1}{L} \sum_{i=1}^L s_i s_i^{*T} \quad (15)$$

where  $s_i$  denotes the single-look scattering vector, which equals  $s_{part}$  in the case of partial POLSAR and  $s_{full}$  in the case of full polarimetry, and  $L$  is the number of looks.

Complex Wishart distribution statistics, however, are normally written for the scaled covariance matrix  $Z = LC_v$ , whose PDF is given as:

$$pdf(Z; d, \Sigma, L) = \frac{|Z|^{L-d}}{|\Sigma|^L \Gamma_d(L)} e^{-tr(\Sigma^{-1} Z)} \quad (16)$$

with  $\Gamma_d(L) = \pi^{d(d-1)/2} \prod_{i=0}^{d-1} \Gamma(L - i)$  and  $d$  is the dimensional number of the POLSAR covariance matrix.

The approach taken in this paper differs by applying the homoskedastic log transformation on a less-than-well-known result for the determinant of the covariance matrix. Goodman [18] proved that the ratio between the observable and expected values of the sample covariance matrix's determinants behave like a product of  $d$  chi-squared random variables with different degrees of freedom

$$\chi_L^d = (2L)^d \frac{|C_v|}{|\Sigma_v|} \sim \prod_{i=0}^{d-1} \chi^2(2L - 2i) \quad (17)$$

Its log-transformed variable consequently behaves like a summation of  $d$  log-chi-squared random variables with the same degrees of freedom

$$\Lambda_L^d = \ln \left[ (2L)^d \frac{|C_v|}{|\Sigma_v|} \right] \sim \sum_{i=0}^{d-1} \Lambda^\chi(2L - 2i) \quad (18)$$

with  $\Lambda^\chi(k) \sim \ln [\chi^2(k)]$

### B. Original Heteroskedastic Domain and the Homoskedastic Log-Transformation

In this section the multiplicative nature of POLSAR data is first illustrated. Log-transformation is then used to convert the data into a more familiar additive model. Heteroskedasticity, which is defined as the dependence of variance upon the underlying signal, is shown to be the case for the original POLSAR data. In log-transformed domain, the case for a homoskedastic model, where sample variance is fixed and thus independent of the underlying signal, is demonstrated. To keep the section flowing, the mathematical derivation is only presented here in major sketches. For more detailed derivation, Appendix A should be referred to.

From Eqns. 17 and 18 we can deduce the following relationships:

$$|C_v| \sim |\Sigma_v| \cdot \frac{1}{(2L)^d} \cdot \prod_{i=0}^{d-1} \chi^2(2L - 2i) \quad (19)$$

$$\ln |C_v| \sim \ln |\Sigma_v| - d \cdot \ln(2L) + \sum_{i=0}^{d-1} \Lambda(2L - 2i) \quad (20)$$

In a given homogeneous POLSAR area, the parameters  $\Sigma_v$ ,  $d$  and  $L$  can be considered as constant. Thus Eqn. 19 gives the theoretical explanation that: in the original POLSAR domain, a multiplicative speckle noise pattern is present. At the same time, Eqn. 20 shows that the logarithmic transformation has converted this to the more familiar additive noise.

Since chi-squared random variables  $X \sim \chi^2(k)$  follows a known PDF:

$$pdf(x; 2L) = \frac{x^{L-1} e^{-x/2}}{2^L \Gamma(L)} \quad (21)$$

applying the variable change theorem, its log-transformed variable follows the PDF of:

$$pdf(x; 2L = k) = \frac{e^{Lx - e^x/2}}{2^L \Gamma(L)} \quad (22)$$

As the PDFs become available, the characteristic functions (CF) of both the chi-squared and log-chi-squared random variables can be written as:

$$CF_\chi(t) = (1 - 2it)^L \quad (23)$$

$$CF_\Lambda(t) = 2^{it} \frac{\Gamma(L + it)}{\Gamma(L)} \quad (24)$$

Subsequently their means and variances can be computed from the given characteristic functions.

They are:

$$\text{avg} [\chi(2L)] = 2L \quad (25)$$

$$\text{var} [\chi(2L)] = 4L \quad (26)$$

$$\text{avg} [\Lambda(2L)] = \psi^0(L) + \ln 2 \quad (27)$$

$$\text{var} [\Lambda(2L)] = \psi^1(L) \quad (28)$$

where  $\psi^0()$  and  $\psi^1()$  represent the digamma and trigamma functions respectively.

Since the average and variance of both chi-squared distribution and log-chi-squared distribution are constant, the product and summation of these random variables also has fixed summary statistics. Specifically:

$$\begin{aligned} \text{avg} \left[ \prod_{i=0}^{d-1} \chi^2(2L - 2i) \right] &= 2^d \cdot \prod_{i=0}^{d-1} (L - i), \\ \text{var} \left[ \prod_{i=0}^{d-1} \chi^2(2L - 2i) \right] &= \prod_{i=0}^{d-1} 4(L - i)(L - i + 1) - \prod_{i=0}^{d-1} 4(L - i)^2, \\ \text{avg} \left[ \sum_{i=0}^{d-1} \Lambda(2L - 2i) \right] &= d \cdot \ln 2 + \sum_{i=0}^{d-1} \psi^0(L - i), \\ \text{var} \left[ \sum_{i=0}^{d-1} \Lambda(2L - 2i) \right] &= \sum_{i=0}^{d-1} \psi^1(L - i) \end{aligned}$$

Combining these results with Eqns. 19 and 20, we have:

$$\text{avg} [|C_v|] = \frac{|\Sigma_v|}{L^d} \prod_{i=0}^{d-1} (L - i) \quad (29)$$

$$\text{var} [|C_v|] = \frac{|\Sigma_v|^2 \left[ \prod_{i=0}^{d-1} (L - i)(L - i + 1) - \prod_{i=0}^{d-1} (L - i)^2 \right]}{L^{2d}} \quad (30)$$

$$\text{avg} [\ln |C_v|] = \ln |\Sigma_v| - d \cdot \ln L + \sum_{i=0}^{d-1} \psi^0(L - i) \quad (31)$$

$$\text{var} [\ln |C_v|] = \sum_{i=0}^{d-1} \psi^1(L - i) \quad (32)$$

For a real world captured image, while the parameters  $d$  and  $L$  do not change for the whole image, the underlying  $\Sigma_v$  is expected to differ from one region to the next. Thus over

an heterogeneous scene, the stochastic process for  $|C_v|$  and  $\ln |C_v|$  varies depending on the underlying signal  $\Sigma_v$ . In such context, Eqn. 30 implies that the variance of  $|C_v|$  also differs depending on the underlying signal  $\Sigma_v$ , which indicates its heteroskedastic property. At the same time, in the log-transformed domain, Eqn. 32 reveals that the variance of  $\ln |C_v|$  is invariant and independent of  $\Sigma_v$  manifesting its homoskedastic nature.

### C. Consistent Measures of Distance for POLSAR

Similar to the way dispersion and contrast is defined in our previous work [19] [20], this section introduces the consistent sense of distance from a couple of different perspectives. Assuming, on the one hand, that the true value of the underlying signal  $\Sigma_v$  is known *a priori*, random variables, ratio ( $\mathbb{R}$ ) and log-distance ( $\mathbb{L}$ ), are observable according to their definitions:

$$\mathbb{R} = \frac{|C_v|}{|\Sigma_v|} \quad (33)$$

$$\mathbb{L} = \ln |C_v| - \ln |\Sigma_v| \quad (34)$$

On the other hand, under a more forgiving assumption where the POLSAR is known to have come from a homogeneous area, but the true value of the underlying signal  $\Sigma_v$  is *unknown*, the dispersion ( $\mathbb{D}$ ) and contrast ( $\mathbb{C}$ ) random variables are observable and they are defined as:

$$\mathbb{D} = \ln |C_v| - \text{avg}(\ln |C_v|) \quad (35)$$

$$\mathbb{C} = \ln(|C_{v1}|) - \ln(|C_{v2}|) \quad (36)$$

Using the results from Eqns. 19, 20 and 31 we have

$$\mathbb{R} \sim \frac{1}{(2L)^d} \cdot \prod_{i=0}^{d-1} \chi^2(2L - 2i) \quad (37)$$

$$\mathbb{L} \sim \sum_{i=0}^{d-1} \Lambda(2L - 2i) - d \cdot \ln(2L) \quad (38)$$

$$\mathbb{D} \sim \sum_{i=0}^{d-1} \Lambda(2L - 2i) - d \cdot \ln 2 + k \quad (39)$$

$$\mathbb{C} \sim \sum_{i=0}^{d-1} \Delta(2L - 2i) \quad (40)$$

with  $\Delta(2L) \sim \Lambda(2L) - \Lambda(2L)$  and  $k = \sum_{i=0}^{d-1} \psi^0(L - i)$

Also given the characteristic functions (CF) for the elementary components  $\Lambda(2L)$  written in Eqn. 24, Appendix B derives the characteristic functions for the summative random variables as:

$$CF_{\Lambda_L^d}(t) = \frac{2^{idt}}{\Gamma(L)^d} \prod_{j=0}^{d-1} \Gamma(L - j + it) \quad (41)$$

$$CF_{\mathbb{L}}(t) = \frac{1}{L^{idt} \Gamma(L)^d} \prod_{j=0}^{d-1} \Gamma(L - j + it) \quad (42)$$

$$CF_{\mathbb{D}}(t) = \frac{e^{ikt}}{\Gamma(L)^d} \prod_{j=0}^{d-1} \Gamma(L - j + it) \quad (43)$$

$$CF_{\Delta(2L)} = \frac{\Gamma(2L)B(L - it, L + it)}{\Gamma(L)^2} \quad (44)$$

$$CF_{\mathbb{C}}(t) = \prod_{j=0}^{d-1} \frac{\Gamma(2L - 2j)B(L - j - it, L - j + it)}{\Gamma(L - j)^2} \quad (45)$$

Since each elementary component follows fixed distributions (i.e.  $\chi^2(2L), \Lambda(2L), \dots$ ), it is natural that these variables also follow fixed distributions. Moreover, they are independent of  $\Sigma_v$ . In short, these random variables are shown to follow consistent and fixed distributions, regardless of the underlying signal  $\Sigma_v$ .

#### IV. SAR AS THE SPECIAL CASE OF POLARIMETRIC SAR

The previous section has introduced the theoretical model for 3-dimensional  $d = 3$  full polarimetric and two dimensional  $d = 2$  partial polarimetry cases. In this section, the model is shown to be also applicable for the 1-dimensional  $d = 1$  case. Physically this means the multi-dimensional POLSAR dataset is collapsed into one-dimensional conventional SAR data. Mathematically, the sample covariance matrix is reduced to the sample variance and the determinant equates the scalar value. On the other hand, it is well known that for SAR data, variance equals intensity. Thus the special case of our result is investigated carefully and is shown to be consistent with previous results for SAR intensity data. This can be thought of either as a cross-validation evidence for the proposed POLSAR models or alternatively as having SAR as the special case of POLSAR.

The results so far for our models can be summarized using the following equations:

$$\mathbb{R} = \frac{|C_v|}{|\Sigma_v|} \sim \frac{1}{(2L)^d} \prod_{i=0}^{d-1} \chi^2(2L - 2i) \quad (46)$$

$$\mathbb{L} = \ln |C_v| - \ln |\Sigma_v| \sim \sum_{i=0}^{d-1} \Lambda(2L - 2i) - d \cdot \ln 2L \quad (47)$$

$$\mathbb{D} = \ln |C_v| - \text{avg}(\ln |C_v|) \sim \sum_{i=0}^{d-1} \Lambda(2L - 2i) - d \ln 2 + k \quad (48)$$

$$\mathbb{C} = \ln |C_{1v}| - \ln |C_{2v}| \sim \sum_{i=0}^{d-1} \Delta(2L - 2i) \quad (49)$$

$$\mathbb{A} = \text{avg}(\mathbb{L}) = \sum_{i=0}^{d-1} \psi^0(L - i) - d \cdot \ln L \quad (50)$$

$$\mathbb{V} = \text{var}(\mathbb{L}) = \sum_{i=0}^{d-1} \psi^1(L - i) \quad (51)$$

$$\mathbb{E} = \text{mse}(\mathbb{L}) = \left[ \sum_{i=0}^{d-1} \psi^0(L - i) - d \cdot \ln L \right]^2 + \sum_{i=0}^{d-1} \psi^1(L - i) \quad (52)$$

Upon setting  $d = 1$  into the above equations, Appendix C shows that the reduced results are consistent with the following two cases. First is the the following results obtained from the our previous works on single-look SAR [19] [20], i.e.  $d = L = 1$ ,

$$I \sim \bar{I} \cdot \text{pdf} [e^{-R}]$$

$$\log_2 I \sim \log_2 \bar{I} + \text{pdf} [2^x e^{-2^x} \ln 2]$$

$$\mathbb{R} = \frac{I}{\bar{I}} \sim \text{pdf} [e^{-x}]$$

$$\mathbb{L} = \log_2 I - \log_2 \bar{I} \sim \text{pdf} [2^x e^{-2^x} \ln 2]$$

$$\mathbb{D} = \log_2 I - \text{avg}(\log_2 I) \sim \text{pdf} [e^{-(2^x e^{-\gamma})} 2^x e^{-\gamma} \ln 2]$$

$$\mathbb{C} = \log_2 I_1 - \log_2 I_2 \sim \text{pdf} \left[ \frac{2^x}{(1 + 2^x)^2} \ln 2 \right]$$

$$\mathbb{A} = \text{avg}(\mathbb{L}) = -\gamma / \ln 2$$

$$\mathbb{V} = \text{var}(\mathbb{L}) = \frac{\pi^2}{6} \frac{1}{\ln^2 2}$$

$$\mathbb{E} = \text{mse}(\mathbb{L}) = \frac{1}{\ln^2 2} (\gamma^2 + \pi^2/6) = 4.1161$$



The second is the following well-known results for multi-look SAR, i.e.  $d = 1, L > 1$ :

$$I \sim pdf \left[ \frac{L^L x^{L-1} e^{-Lx/\bar{I}}}{\Gamma(L) \bar{I}^L} \right] \quad (53)$$

$$N = \ln I \sim pdf \left[ \frac{L^L}{\Gamma(L)} e^{L(x-\bar{N}) - L e^{x-\bar{N}}} \right] \quad (54)$$

Furthermore, the following derivations for multi-look SAR data show that it can be thought of either as extensions of the corresponding single-look SAR results or as simple cases of the POLSAR results are also derived as:

$$\begin{aligned} \mathbb{R} = \frac{I}{\bar{I}} &\sim pdf \left[ \frac{L^L x^{L-1} e^{-Lx}}{\Gamma(L)} \right] \\ \mathbb{L} = \ln I - \ln \bar{I} &\sim pdf \left[ \frac{L^L e^{Lt - Le^t}}{\Gamma(L)} \right] \\ \mathbb{D} = \ln I - avg(\ln I) &\sim pdf \left[ \frac{e^{L[x - \psi^0(L)] - e^{[x - \psi^0(L)]}}}{\Gamma(L)} \right] \\ \mathbb{C} = \ln I_1 - \ln I_2 &\sim pdf \left[ \frac{e^x}{(1 + e^x)^2} \right] \\ \mathbb{A} = avg(\mathbb{L}) &= \psi^0(L) - \ln L \\ \mathbb{V} = var(\mathbb{L}) &= \psi^1(L) \\ \mathbb{E} = mse(\mathbb{L}) &= [\psi^0(L) - \ln L]^2 + \psi^1(L) \end{aligned}$$

This newly derived models for multi-look SAR data can also be validated against real-life data. Fig. 1 presents the results of an experiment carried out for the stated purpose. In the experiment the intensity of a single-channel SAR data (HH) for a homogeneous area in the AIRSAR Flevoland dataset is extracted. The histograms for the log-distance and contrast is then plotted against the theoretical PDF given above. The plot is obtained with ENL set to the nominal number of 4, and good visual match is apparent in the final results.

## V. VALIDATING THE MODELS AGAINST REAL-LIFE DATA

This section validates the theoretical models developed above against real-life practical data. The first sub-section provides a naive validation, where the nominal ENL is used for the model. While the match appears to be reasonably good, it can be further improved. After the second sub-section discusses why the nominal look-number given by (POL)SAR processors may not be

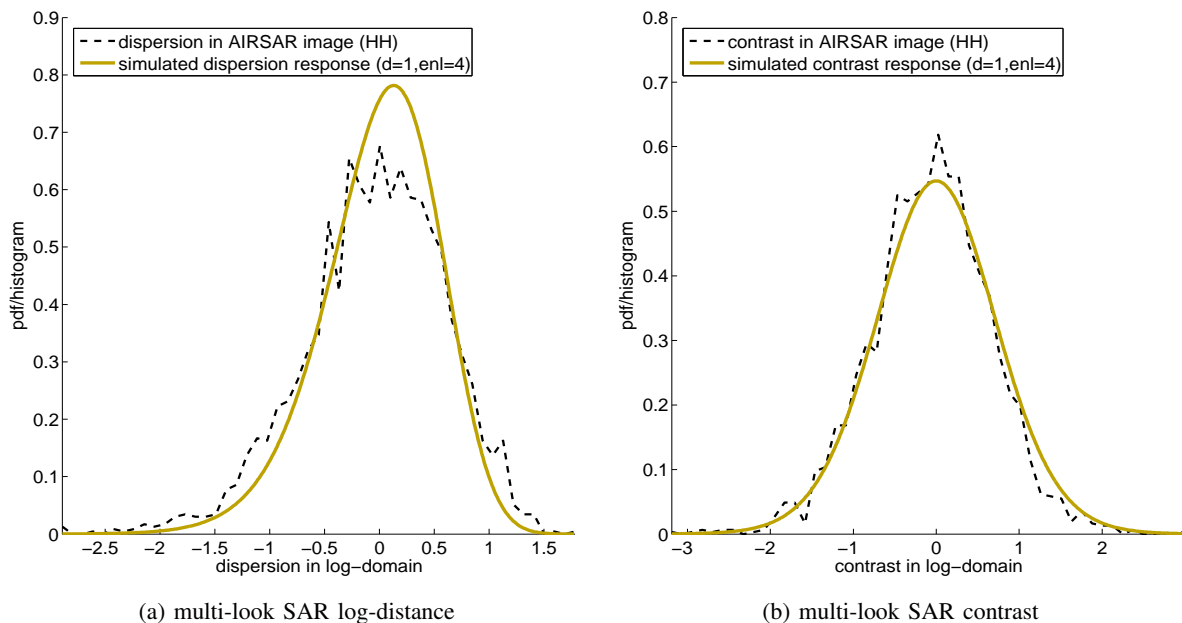


Fig. 1: Multi-Look SAR dispersion and contrast: modelled response matches very well with real-life captured data.

very accurate, the third sub-section proposes a new technique in estimating the Effective Number of Looks (ENL) using the consistent variance found in homoskedastic model. With the newly estimated ENL, the final sub-section shows that the match between the theoretical model and the practical data is indeed further improved.

#### A. Using the nominal ENL to validate the theoretical models

This sub-section describes an experiment to validate the models presented earlier against real-life captured data, which can be performed in a rather straightforward manner as follows. The stochastic models derived in the previous sections can be graphically visualized as histogram plots of the simulated data. At the same time, the form of the real-life practical data is also observable via the histogram plots of the data samples extracted from an homogeneous area. Therefore, the theoretical models can be validated if for the same parameters the two plots match each other reasonably well.

For this purpose, a homogeneous area was chosen from the AIRSAR Flevoland POLSAR data as experimental data samples. Then theoretical models are used to explain the data. The validating

models include: the determinant and its log-transformed models, together with the dissimilarity measures namely: the determinant ratio, log-distance, dispersion and the contrast measures of distance.

These models are closely related as follows. For the same parameter set, the determinant and determinant ratio are simply scaled versions of each other. Meanwhile, the log-determinant, log-distance and dispersion are also just shifted versions of each other. Hence one could expect that once a model is validated, the other models in the set will follow suit, assuming that all the parameters of the image are known. Nevertheless, all the models will be separately evaluated in this section.

Among all these models, the least-assumed stochastic process for dispersion and contrast measures of distance are validated first. For each pixel in the region, the determinant of the covariance matrix is computed and the log-transformation is applied. Then the average of POLSAR covariance matrixs determinant in the log-transformed domain, i.e.  $avg(\ln|C_v|)$ , is measured for dispersion. Subsequently the observable samples of dispersion and contrast are computed according to Eqns. 35 and 36 in order to plot their histograms.

Similarly, theoretical simulations according to Eqns. 39 and 40 are carried out.  $L = 4$  for this study, while the dimensional number is set to either 3 or 2 depending on whether a full or partial polarimetric SAR dataset is being investigated. The plots are presented in Fig. 2 showing an evident visual match between the model and real data, thus effectively validating the theoretical models for dispersion and contrast measures of distance.

Apart from dispersion and contrast, the other four models to be investigated require an estimation of the “true” underlying signal  $|\Sigma_v|$ . There are two ways to estimate this quantity over an homogeneous area. The traditional way is to simply set the true signal equal to the average of the POLSAR covariance matrix in its original domain, i.e.  $\Sigma_v = avg(C_v)$ . Another approach is to estimate the true signal from the average of the log-determinant of the POLSAR covariance matrix (i.e.  $avg[\ln|C_v|]$ ) using Eqn. 31. Both approaches will be presented in this section. As the log-determinant average has already been computed earlier, the second approach is hence used first for the validation of determinant-ratio and log-distance.

Fig. 3 plots the determinant-ratio and log-distance models against real-life data. In this experiment, the theoretical models are simulated using Eqns 37 and 38, while the observable samples are computed using Eqns 33 and 34 with the true signal estimated from the log-

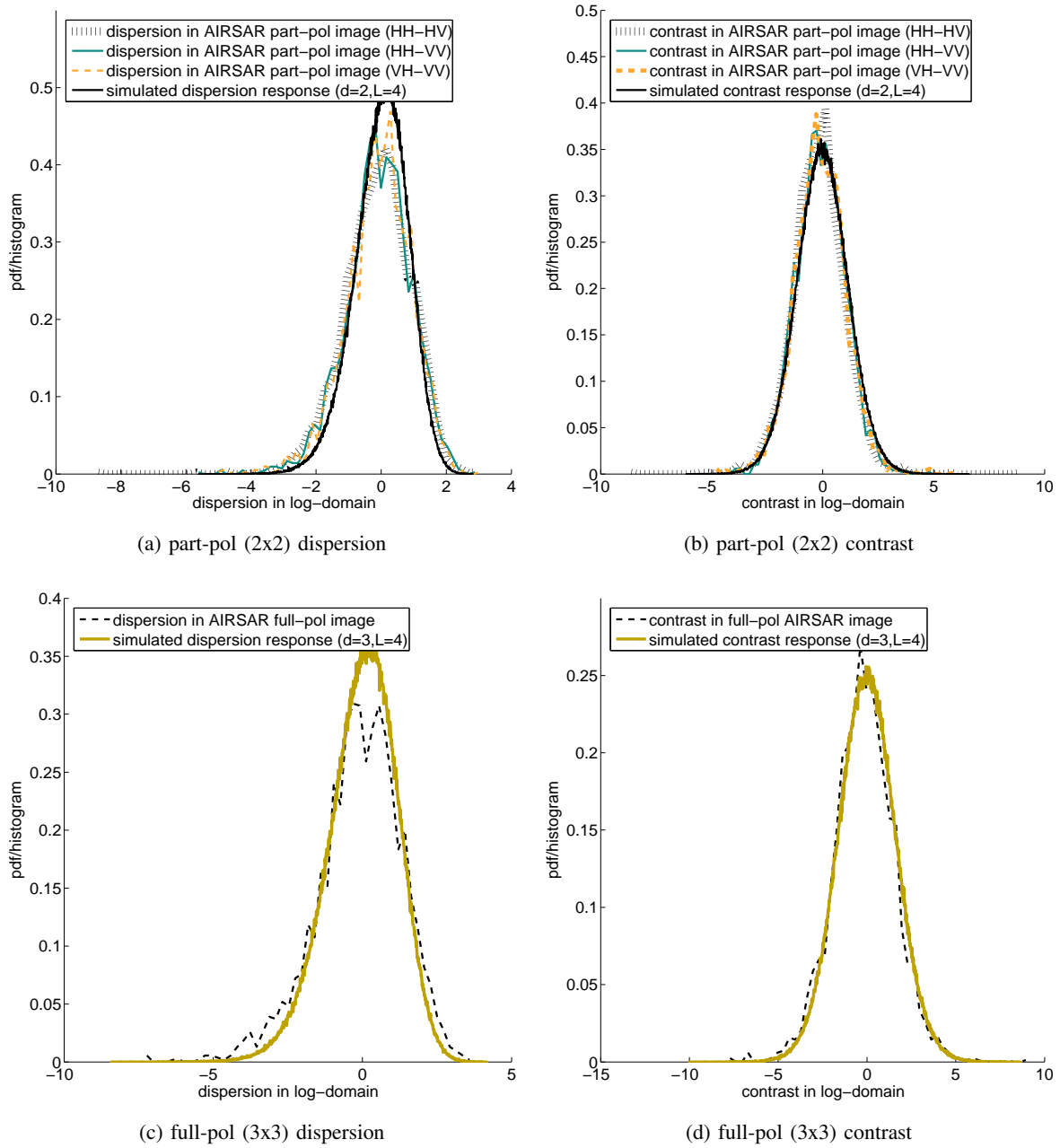


Fig. 2: Validating the dispersion and contrast models against both partial and full polarimetric AIRSAR Flevoland data.

determinant average, i.e.  $avg(\ln |C_v|)$ . A reasonable match is again observed which validates the models for log-distance and determinant ratio.

Since the models for the determinant and log-determinant are just scaled or shifted version of

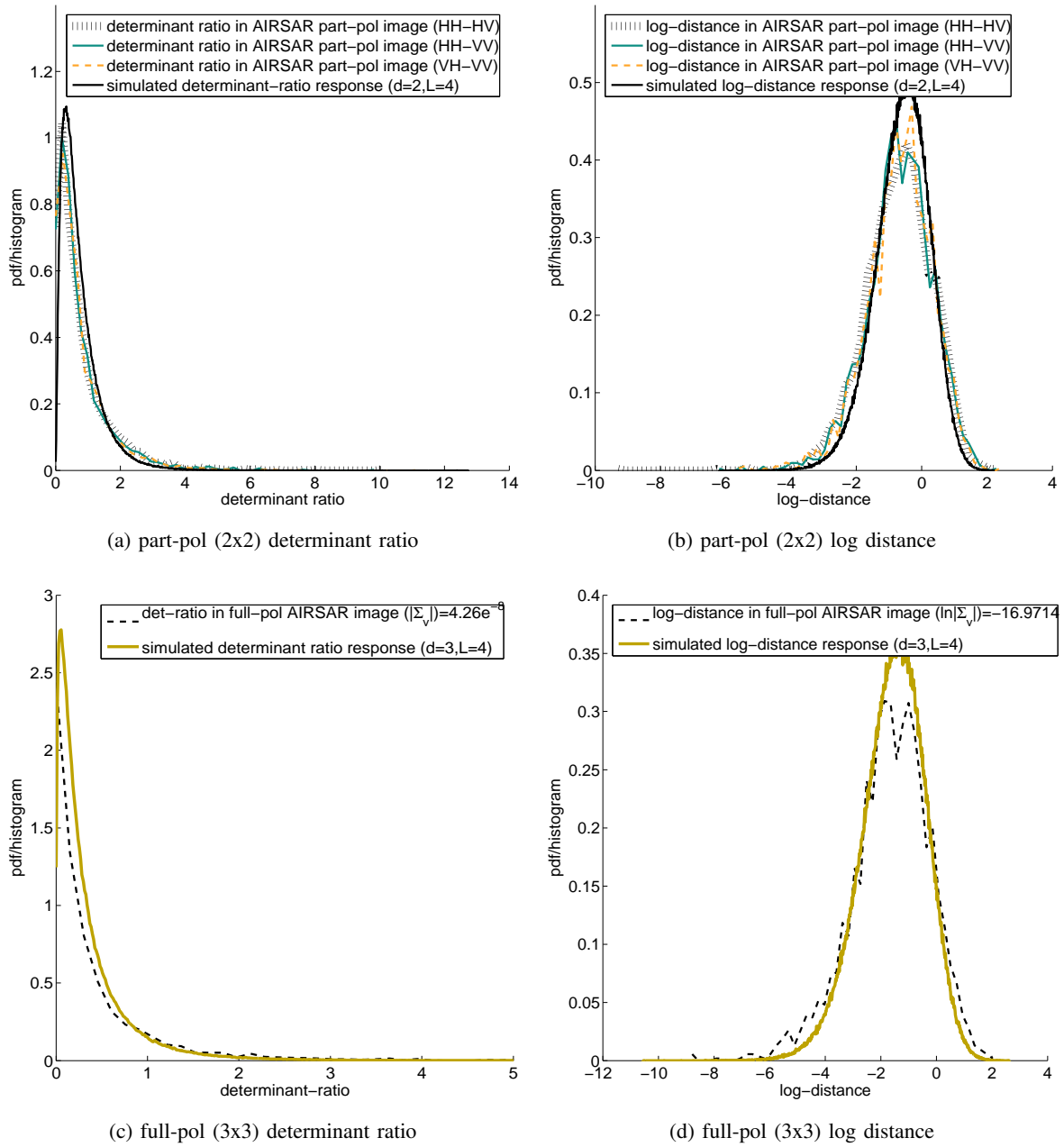


Fig. 3: Validating determinant-ratio and log-distance models with  $|\Sigma_v|$  is computed using  $avg(\ln |C_v|)$

the models for determinant-ratio and log-distance, similar validation results are to be expected.

However, a more subtle observation phenomena occurs during the validation process for the determinant and its log-transformed model, where the theoretical response is taken from the

simulated stochastic process described by Eqns. 19 and 20. The phenomena happens when the true signal is estimated by the first approach i.e. equal to the average of the sample covariance matrix in its original domain (which evidently results in a different estimation for the true signal when compared with the method applied earlier).

Subsequently the validation plots, which are presented in Fig 4, exhibit some small translation and scaling discrepancies – which are easier to observe in the log-determinant plots. Despite this, the curve shapes are quite similar.

In short the least-assumed dispersion and contrast measures of distance are shown to match reasonably well with the practical data. The same can be stated for the other four models, namely: determinant, log-determinant, determinant ratio and log-distance, if the underlying parameters can be estimated reasonably well for the given image. However as described above a single “true signal”  $|\Sigma_v|$  can have two different estimated values, depending on which estimation method was being used. The discrepancy suggests that at least one parameter for the models was inaccurately estimated. In fact, the next sub-section specifically indicates that the nominal look-number given by the (POL)SAR processor may not accurately reflect the true nature of the captured data.

As will be shown in Section V-B, the reason is due to the inappropriate look number being used. Furthermore, the match between the theoretical model and the practical data will also be shown to improve once a more accurate look number (ENL) is estimated. For now, let us simply observe that using appropriate estimation of the parameters, the proposed models match reasonably well with the practical data.

### *B. The difference between the theoretical models and the practical data*

Even though the assumptions made in developing this theory have intentionally been kept minimal, like all other similar models, the proposed model in this paper is built upon certain presumptions. Practical conditions however may not always satisfy these prerequisites. In this section, a common and observable gap between the conditions found in practical real-life data and the theoretical assumptions is discussed. And it is shown that: the theoretical model proposed can apply to the practical data, even when this “imperfection” is taken into account.

The assumption of statistical independence between samples (which applies to both SAR and POLSAR data) is reasonable given that the transmission and receipt of analogue signals is done independently for each radar pulse, i.e. for each resolution cell. Thus, theoretically speaking,

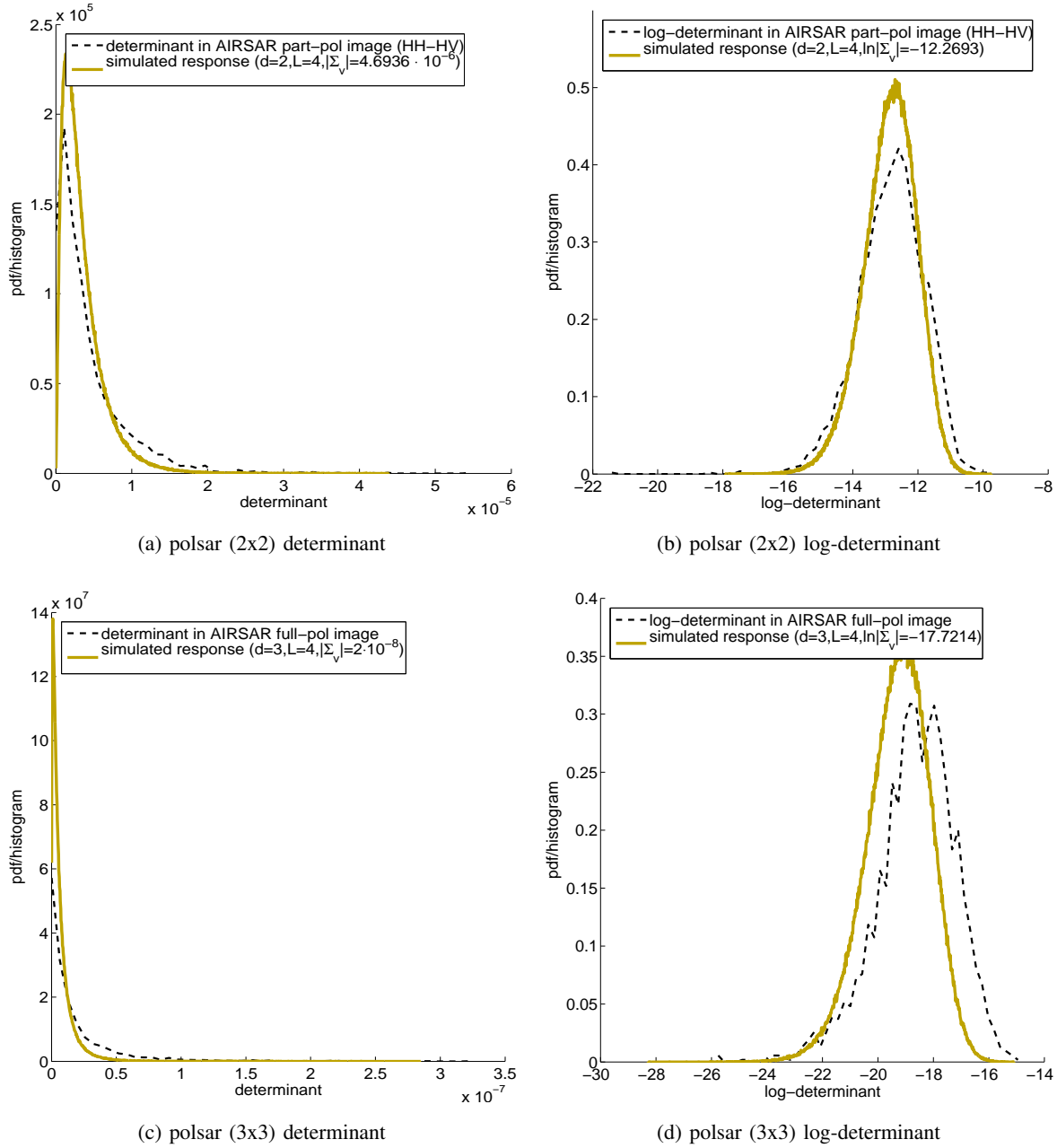


Fig. 4: Validating determinant and log-determinant models with  $\Sigma_v = \text{avg}(C_v)$

adjacent pixels in an image can be assumed to be statistically independent. However, the actual imaging mechanism in a real-life (POL)SAR processor is of a digital nature, where the analogue signal is to be converted into a digital data-set. Specifically, the analogue SAR signal, which is characterised by the pulse bandwidth measurement, is fed into an analogue-to-digital (ADC)

sampling and conversion process which is characterised by its sampling rate. Theoretically it may be possible to define a sampling rate that ensures each digital pixel corresponds exactly to an separate analogue physical cell. Practically however, to ensure “perfect reconstruction”, the sampling rate is normally set at a slightly higher value than the Nyquist rate, resulting in a higher number of samples per pixel than the number of physical cells available in the scene.

Stated differently, in practice, each physical radar cell may be spread over more than a single pixel, resulting in potentially high correlation between neighbouring pixels. This high sampling rate also results in a significantly higher correlation between pairs of pixels that may be related within a single physical cell resolution. Then the correlation found between pairs of pixels that are further away and hence having less physical relation to each other will increase. It also results in reduced effective number of look, such as for a window of  $3 \times 3$  pixels, it actually contains less than 9 physical analogue cells. The former phenomena is partially explained in [21] for SAR, while the later is experimental observed for POLSAR data in [14] and [22]. The oversampling practice is also documented by the producers of SAR processors. For AIRSAR, the sampling rate and pulse bandwidth combinations are either 90/40MHz or 45/20MHz [23]. While for RadarSat2, the pixel resolution and range - azimuth resolutions for SLC fine-quad mode is advertised as  $(4.7 \cdot 5.1)m^2 / (5.2 \cdot 7.7)m^2$  [24]

The proposed model can handle this imperfection that is found in practical data. The trick is that instead of using the nominal Number of Looks given by the SAR processor, an ENL estimation procedure is first undertaken, and then the obtained ENL used subsequently. The first part of this section details a simple ENL estimation technique for POLSAR data. While the second part demonstrates how the practical imperfection manifest itself and how it can be handled in a RADARSAT2 dataset. It also illustrates how the match shown in Section V for the AIRSAR Flevoland dataset can be improved using ENL estimation.

### C. ENL Estimation

The common approach in ENL estimation is to investigate the summary statistics of a known homogeneous area in the given data before making inferences about the inherent ENL. The summary statistics for  $|C_v|$  and  $\ln |C_v|$  have been derived in Section III-B, where Eqn. 31 indicates that there is a relationship among  $|avg(C_v)|$ ,  $avg(\ln |C_v|)$ ,  $d$ ,  $L$ . Recall that in carrying out the validation process using AIRSAR Flevoland data with nominal value  $L = 4$ , the relationship



was shown to be broken. The reason is believed to be in the use of inexact value for  $L$ . In a given POLSAR dataset, since all values of  $|avg(C_v)|$ ,  $avg(\ln |C_v|)$ ,  $d$  are known, it is possible to estimate the “effective” number of look, by finding an  $L$  that ensures the above relationship is valid.

In fact, this approach was taken in [22], where an equation of exactly the same form as Eqn. 31 was used to estimate the ENL. Unfortunately, the only known way to solve the equation for the unknown  $L$  requires the use of an “iterative numerical method”. Instead of relying on the equations for statistical mean to find ENL, we propose an approach that makes use of variance statistics in the homoskedastic log-domain to find ENL. Specifically, Eqn. 32 can be rewritten as:

$$var[\ln |C_v|] = f(L) = \sum_{i=0}^{d-1} \psi^1(L - i) \quad (55)$$

where  $\psi^1()$  again denotes the tri-gamma function.

Thus theoretically, given some measurable value for  $var[\ln |C_v|]$ , one could solve the above equation for the unknown  $L$ , which would also require some iterative computations. Practically however, the shape of the right-hand-side can be pre-computed and for each computed value of  $var[\ln |C_v|]$ , a corresponding value for  $L$  can be found by referencing the variance value on the pre-computed graph or by using the following equation:

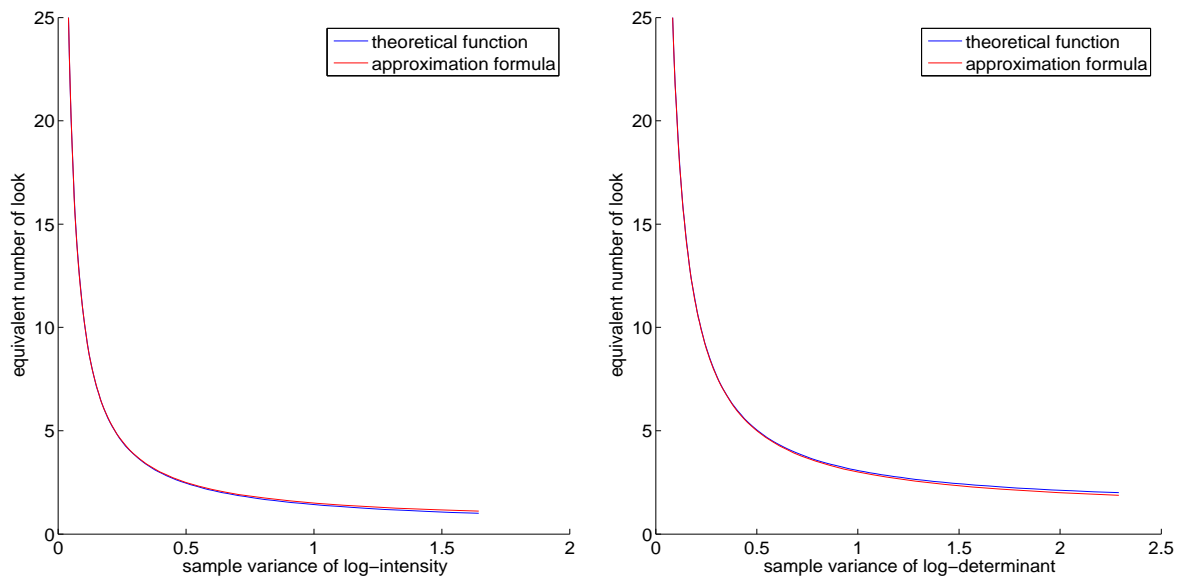
$$\hat{L} = d \left( \frac{1}{var(\ln |C_v|)} + 0.5 \right) \quad (56)$$

Fig. 5 shows the shapes of the function defined in Eqn. 55 for SAR and partial-POLSAR data  $f_{d=1}(L)$  and  $f_{d=2}(L)$  as well as illustrating the simplified approximation formula (Eqn. 56).

#### D. Using estimated ENL to better explain practical data

For this experiment an example RADARSAT2 dataset is used, in its Fine-Quad mode Single-Look format. Nine-look processing is applied before the dispersion histogram in the log-transformed domain is computed for a known homogeneous area. The histograms for both one-dimensional SAR and two-dimensional partial POLSAR data are plotted in Fig. 6 against the theoretical models for the nominal ENL value of 9. The match, however, is evidently not very close.

A better match can be achieved by first estimating ENL from the observable variance of the log-determinant, and the theoretical model is then simulated for the estimated ENL. Then the



(a) ENL and variance log-intensity relations for SAR data (b) ENL and var(log-det) relations for partial POLSAR data

Fig. 5: The relations between ENL and sample variance of log-determinant/log-intensity

new sample histogram is plotted in the same figure, showing a much better consistency. This procedure can always be carried out for a given dataset, as long as a homogeneous area can be defined and extracted.

Fig. 7 shows that the over-sampling issue is also present in the AIRSAR Flevoland dataset, even though it is to a much lesser-extent. Still, the “corrected” ENL offers an evidently better match between the model and real-life data. The mis-match problem appears to depend upon how much over-sampling was used to generate the dataset as well as upon the data dimension.

## VI. EVALUATING POLSAR SPECKLE FILTERS USING THE CONSISTENT MEASURES OF DISTANCE

Previous sections have developed a model for POLSAR, which is also shown to be applicable to SAR. In this section, the use of consistent measures of distance in the context of POLSAR speckle filtering are explored briefly. It has been found [25] that for SAR data in its original domain, ratio is a better evaluation than standard subtractive residual. However, ratio residual is argued as not being natural for digital display [26]. Our previous work in the context of SAR speckle filtering found that in the log-transformed domain, this ratio is transformed into a

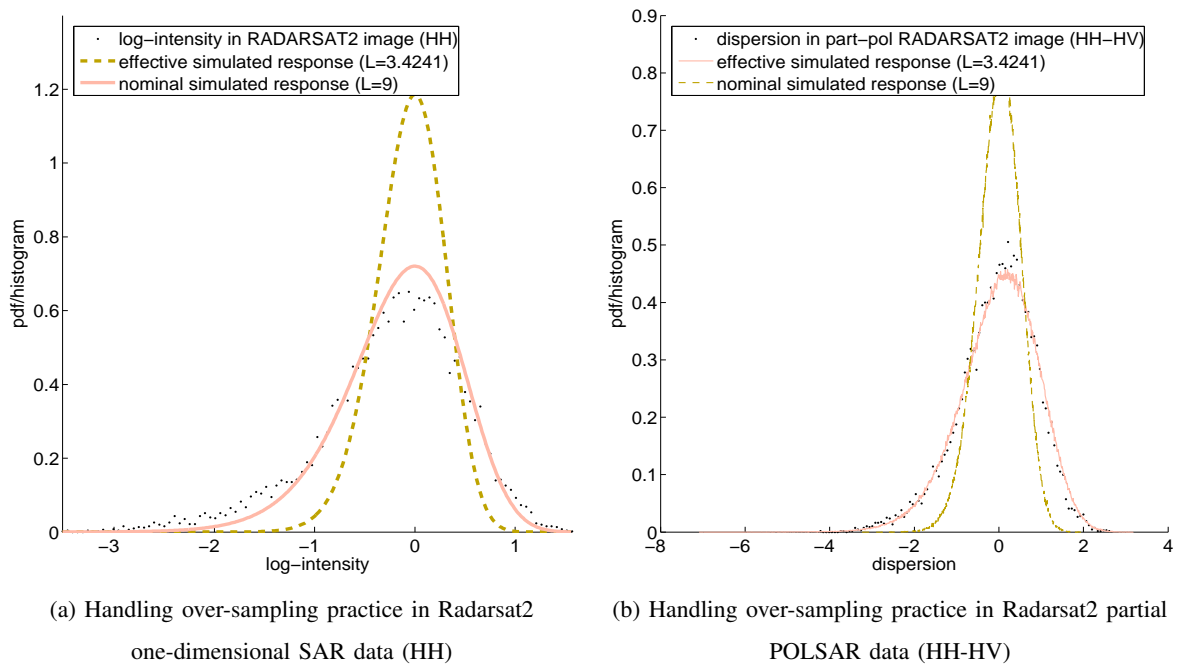


Fig. 6: 9-look processed Radarsat2 data do not exactly exhibit 9-look data characteristics. Homoskedastic model in log-transformed domain can successfully estimate the effective ENL and then explain the data reasonably well.

subtractive residual that is homoskedastic.

The variance of sample log-determinant is shown to be linked to the ENL index. This forms the basis for evaluating POLSAR speckle filters over homogeneous areas. The procedure is simple: To evaluate a given POLSAR speckle filter over homogeneous areas, the filter is applied over a known homogeneous area and the sample variance of log-determinant is measured. The Equivalent Number of Looks (ENL) is then estimated either by referencing prepared graphs from Eqn. 55 or alternatively by setting the measured variance value to  $var[\ln |C_v|]$  in Eqn. 56.

In order for such a procedure to be generic, it is important that the given POLSAR speckle filter preserve the consistency property in the log-transformed domain. That can be tested by applying the POLSAR filter into different sets of homogeneous areas and investigating the plots of the dissimilarity measures presented above. Fig. 8 presents two example plots to show that the  $3 \times 3$  POLSAR boxcar filter preserves the consistency property. In this case, the boxcar filter is applied to 2 sets of part-pol AIRSAR data over Flevoland (HH-HV and VH-VV). Log-determinant and

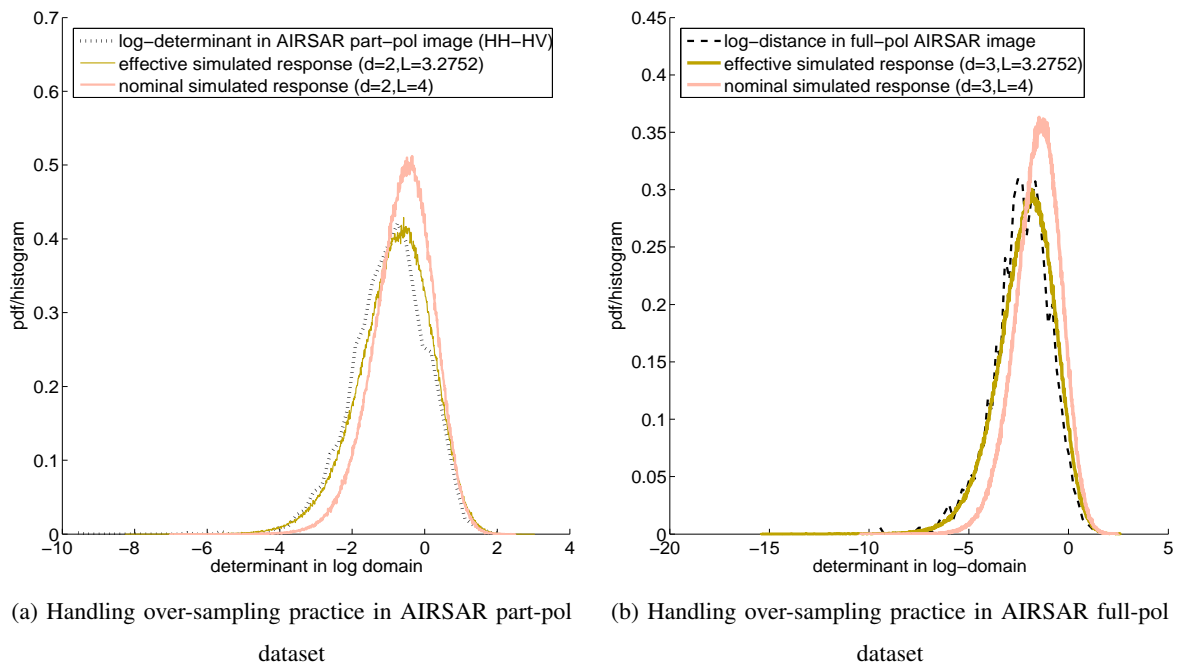


Fig. 7: AIRSAR Flevoland also exhibits phenomena of over-sampling practice, through at a lesser extend than the RADARSAT 2 data.

the contrast measures are computed for the input and output filtered POLSAR data, and their plots are presented. In fact, the test procedure can be applied on any of the models presented above.

The consistency property of a POLSAR speckle filter is important not only to make the estimation of ENL become general enough. It is also to ensure that any classification / detection algorithm which is based on the scalar and consistent measures of distance will work on both pre-filtered and post-filtered data. Otherwise if a POLSAR speckle filter gives different plots for different homogeneous areas, then not only its ENL estimation will be dependent on the underlying signal, but its output also shall not follow the statistical distribution family that characterises multi-look POLSAR. Thus the preservation of this consistency is believed to be an important consideration for POLSAR speckle filters if we want many general detection and classification algorithms to work on the filtered data output.

In evaluation over heterogeneous area, the consistent measures of distance may also be an invaluable tool. Firstly, since the model for log-determinant is additive and homoskedastic, log-

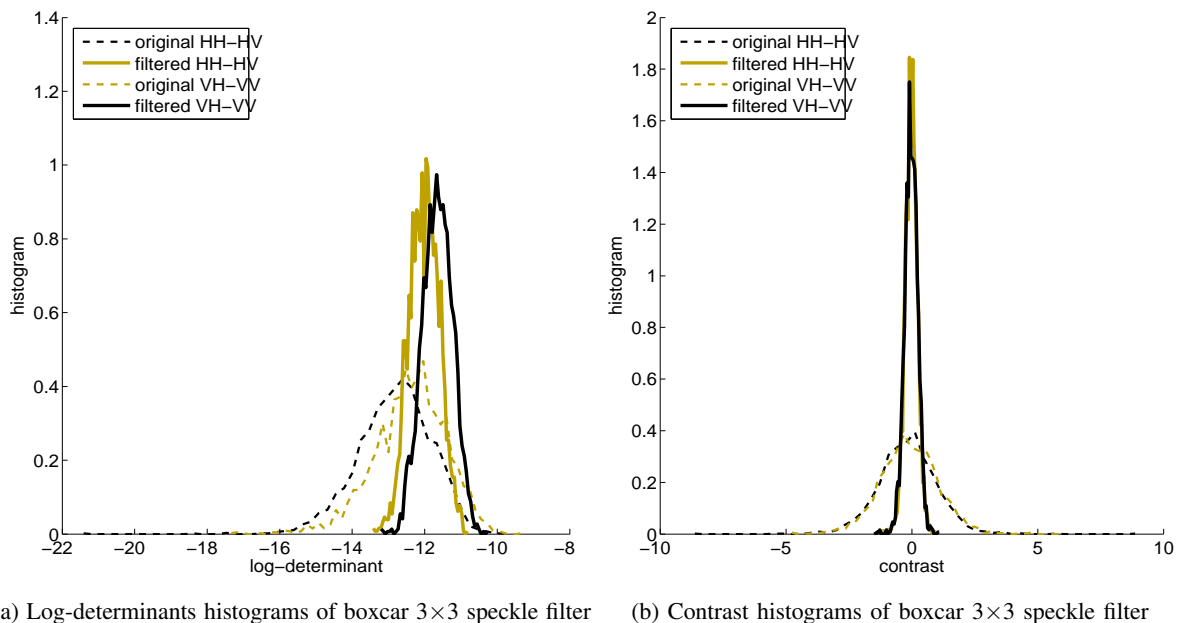


Fig. 8: POLSAR  $3 \times 3$  boxcar filter preserves the consistency property. Consistency means: as long as the area is homogeneous, regardless of the underlying signal  $\Sigma_v$  the shapes of the histograms should be the same.

determinant images may naturally be better suited for gray-level digital display. Specifically for evaluation of statistical estimators, it is both important and convenient to investigate the estimators' error / residual image.

For further analysis, the residual is defined here as the distance between the log-determinants of the filtered outputs and the original input. Ideally speaking, under the context of an additive model, a perfect estimators residual should consist only of random noise. And under the assumption of homoskedasticity, the Gauss Markov theorem becomes applicable. Thus the optimal estimator is expected to exhibit minimal Mean Squared Error (MSE). Over a homogeneous scene, this is reflected in the expectation of minimal bias and variance (hence maximal ENL). Over a heterogeneous scene, where the underlying signal is not known *a priori*, the second best gauge is possibly to have the residual MSE being as close as possible to the MSE of the inherent noise.

To illustrate the above analysis, an experiment is carried out to evaluate the performance of  $3 \times 3$  and  $5 \times 5$  boxcar POLSAR filters on the AIRSAR Flevoland partial polarimetric data (HH-HV). A square  $700 \times 700$  pixel patch is extracted from the AIRSAR dataset, and the two POLSAR

speckle filters applied to the patch. Then the log-determinant images of the filtered outputs are displayed in Fig. 9. At the same time, the residual is computed for both filters, and the images are also displayed in the same figure. Assuming the quantitative evaluation of SAR speckle filters can also be extended to POLSAR speckle filters, the Mean Squared Error (MSE) of the filters residuals are computed and compared with the “optimal” value. This optimal value is computed by setting  $d = 2, L = 4$  into Eqn. C.40 making the expected MSE being  $mse(\mathbb{L}) = 1.0132$ .

Fig. 9 shows that not only does the log-determinant image offer a nice visualization of the scene, but also the distortion impact of the filter can also be made visible by the residual image. In visual evaluation, while it is quite hard to observe the worsening blurring-effects of the boxcar  $5 \times 5$  speckle filter as compared to the  $3 \times 3$  filter in the additive log-determinant image of the filtered output, such a conclusion can be made relatively easier by visualising the residual image.

When quantified evaluation is carried out where the residual MSE is compared with the expected level of noise to be removed, the excessive blurring effects of the  $5 \times 5$  filter become clearly evident. It may be hard to make such a conclusion just by looking at the filtered imagery. However, by investigating the residual between the unfiltered input and the filtered results in the additive and homoskedastic model, both visual and quantitative evaluations offer more conclusive evidence.

Further discussion on the specific topic of evaluating SAR speckle filters is given in our work that focused specifically on SAR [20]. However, due to space restriction, only a brief and critical exploration is explored here for POLSAR speckle filters (i.e. extending the previous SAR approach).

Specifically, this is an illustration of how the proposed theoretical model can possibly be applied to a practical scenario, rather than a full evaluation procedure and methodology.

## VII. DISCUSSION AND CONCLUSION

### A. Discussion

Let us begin the discussion by noting a few theoretical properties of the proposed statistical model. First, the use of covariance matrix log-determinant may be related to the standard eigen-decomposition method of the POLSAR covariance matrices. In fact, the log-determinant can also be computed as the sum of log-eigenvalues. Specifically  $\ln |M| = \sum \ln \lambda_M$  where  $\lambda_M$  denotes all

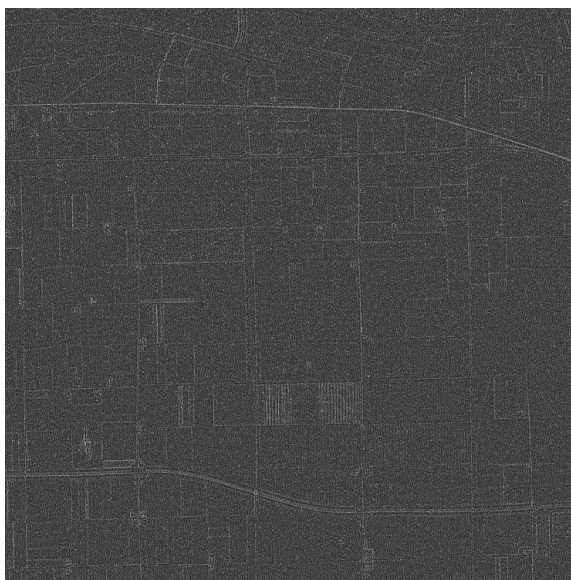
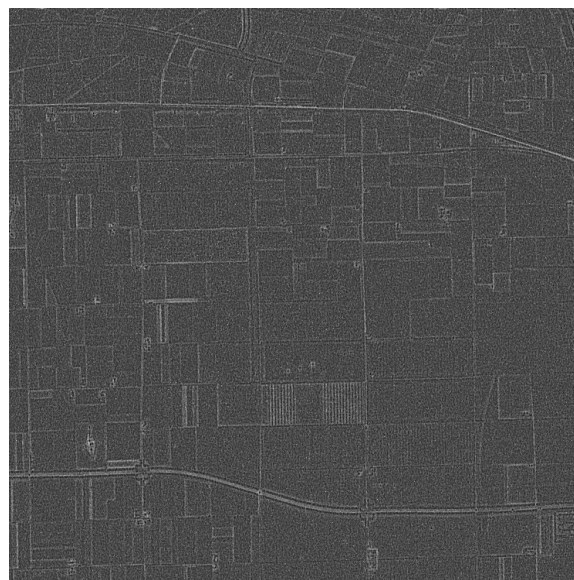
(a) Log-determinant Image of boxcar  $3 \times 3$  speckle filter(b) Log-determinant Image of boxcar  $5 \times 5$  speckle filter(c) Image of Log-determinant Residual for  $3 \times 3$  filter  
(MSE=1.5594)(d) Image of Log-determinant Residual for  $5 \times 5$  filter  
(MSE=2.1420)

Fig. 9: Visually Evaluating POLSAR Boxcar  $3 \times 3$  vs.  $5 \times 5$  Speckle Filters on AIRSAR Flevoland part-pol data (HH-HV) with expected MSE=1.0312 at ENL=4.

the eigenvalues of  $M$ . Thus similar to other eigenvalue based approach (e.g. entropy/anisotropy, ...), the models presented here are invariant to polarization basis transformations.

Second, the model is developed for the POLSAR covariance matrix. However, since the POLSAR coherent matrix is related with the covariance matrix via an unitary transformation, which preserves the determinant as invariant, the model should also be applicable on the coherency matrix.

The model is far from complete. It calls for the reduction of the multi-dimensional POLSAR data into a scalar value. While this is probably desirable for a wide range of application where a one-dimensional number is required to represent the complex multi-dimensional data, such a reduction is unlikely to be lossless. Thus is very similar to the way the Wishart Classifier is employed, and thus to better understand POLSAR data the use of this technique can be complemented with some high-dimensional POLSAR target-decomposition techniques (e.g. the Freeman Durden decomposition [27] or the entropy/anisotropy decomposition [28] ...).

However the model as presented is promising. Those presented in this paper were first developed for partial and monostatic POLSAR data. They were then shown to be also applicable to traditional SAR data. Since the models assumptions are quite minimal, they may also be found to apply to bi-static and interferometric data, although that would require significant further investigations.

The theoretical models may also provide an alternative derivation for the widely used likelihood test statistics in POLSAR. In view of the models given in Eqns 19 & 20, the likelihood test statistics exposed in [1] and rewritten in Eqns 10 & 11 can be simulated as:

$$\ln Q \sim k + L_x \Lambda_{L_x}^d + L_y \Lambda_{L_y}^d - (L_x + L_y) \Lambda_{(L_x+L_y)}^d$$

$$Q \sim e^k \frac{(\chi_{L_x}^d)^{L_x} \cdot (\chi_{L_y}^d)^{L_y}}{(\chi_{L_x+L_y}^d)^{L_x+L_y}}$$

where  $k = d[(L_x + L_y) \ln(L_x + L_y) - L_x \ln L_x - L_y \ln L_y]$ .

Similar to the way that other measures of distance can be used to derive POLSAR classifiers [4], change detectors [1], edge detectors [29] or other clustering and speckle filtering techniques [19] [30], new detection, classification, clustering or speckle filtering algorithms can be derived using the models presented in this paper. Since extensive examples have been shown to support the use of MSE for SAR data, it is reasonable to expect the relevance of MSE to also be demonstrated for POLSAR data. If that is the case, a large number of existing algorithms can become applicable to the POLSAR model in this log-transformed domain, which has been shown to be both additive and homoskedastic.



## B. Conclusion

In conclusion, a couple of statistical models for the determinant of the POLSAR covariance matrix is proposed and validated in this paper. Compared to other statistical models for POLSAR, the proposed models are scalar and representative for the multi-dimensional POLSAR data. These properties lead to the derivation of several statistically consistent discrimination measures for POLSAR. Compared with other discrimination measure proposals, this paper suggests an exact distribution for the POLSAR likelihood statistical test. As a by-product of this exact modelling, simpler dis-similarity measures, i.e. contrast and determinant-ratio, are proposed for the common case of  $Lx = Ly$ .

## APPENDIX A

### HOMOSKEDASTIC MODEL FOR THE LOG-DETERMINANT

#### A. Log-Chi-Square Distribution and its Derivatives

This section provides the mathematical derivations for the log-transformed version of chi-squared random variables.

Chi-squared random variables  $\chi \sim \chi^2(k)$  follows the pdf:

$$pdf(\chi; k) = \frac{\chi^{(k/2)-1} e^{-\chi/2}}{2^{k/2} \Gamma\left(\frac{k}{2}\right)} \quad (\text{A.1})$$

Setting  $L=k/2$  into Eqn. A.1

$$pdf(\chi) = \frac{\chi^{L-1} e^{-\chi/2}}{2^L \Gamma(L)} \quad (\text{A.2})$$

Applying the variable change theorem, which states that: if  $y = \phi(x)$  with  $\phi(c) = a$  and  $\phi(d) = b$ , then:

$$\int_a^b f(y) dy = \int_c^d f[\phi(x)] \frac{d\phi}{dx} dx \quad (\text{A.3})$$

into the log-transformation, which changes the random variables  $\Lambda = \ln(\chi)$ , we have:

$$\begin{aligned} d\chi &= e^\Lambda d\Lambda \\ \frac{\chi^{L-1} e^{-\chi/2}}{2^L \Gamma(L)} d\chi &= \frac{(e^\Lambda)^{L-1} e^{-e^\Lambda/2}}{2^L \Gamma(L)} e^\Lambda d\Lambda \end{aligned}$$

In other words, we have:

$$pdf(\Lambda; L) = \frac{e^{L\Lambda - e^\Lambda/2}}{2^L \Gamma(L)} \quad (\text{A.4})$$

From the PDF given in Eqn. A.4, a characteristic function can be computed. By definition, the characteristic function (CF)  $\varphi_X(t)$  for a random variable  $X$  is computed as:

$$\begin{aligned}\varphi_X(t) = \mathbb{E}[e^{itX}] &= \int_{-\infty}^{\infty} e^{itx} dF_X(x) \\ &= \int_{-\infty}^{\infty} e^{itx} f_X(x) dx\end{aligned}$$

with  $\varphi_X(t)$  is the characteristic function,  $F_X(x)$  is the CDF function of  $X$  and  $f_X(x)$  is the PDF function of  $X$ . Thus the characteristic function for the log-chi-squared distribution is defined as:

$$\varphi_\Lambda(t) = \int_0^\infty e^{itz} \frac{e^{Lx-e^x/2}}{2^L \Gamma(L)} dx \quad (\text{A.5})$$

The Gamma function is defined over the complex domain as:  $\Gamma(z) = \int_0^\infty e^{-x} x^{z-1} dx$ . Thus  $\Gamma(L + it) = \int_0^\infty e^{-x} x^{L+it-1} dx$ . Set  $x = e^z/2$  then  $dx = e^z/2 dz$ , we have  $\Gamma(L + it) = \int_0^\infty e^{itz} \frac{e^{Lz-e^z/2}}{2^{L+it}} dz$

That is:

$$\varphi_\Lambda(t) = 2^{it} \frac{\Gamma(L + it)}{\Gamma(L)} \quad (\text{A.6})$$

Consequently, the first and second derivative of the log-chi-squared distribution can be computed. The first derivative is given as:

$$\frac{\partial \varphi_\Lambda(t)}{\partial t} = \frac{i 2^{it} \Gamma(L + it)}{\Gamma(L)} [\ln 2 + \psi^0(L + it)] \quad (\text{A.7})$$

due to

$$\begin{aligned}\frac{\partial \Gamma(x)}{\partial x} &= \Gamma(x) \psi^0(x), \\ \frac{\partial \Gamma(L + it)}{\partial t} &= i \Gamma(L + it) \psi^0(L + it), \\ \frac{\partial 2^{it}}{\partial t} &= i 2^{it} \ln(2), \\ \partial(u \cdot v)/\partial t &= u \cdot \partial v/\partial t + v \cdot \partial u/\partial t,\end{aligned}$$

where  $\psi^0()$  denotes the di-gamma function.

Meanwhile, the second derivative can be written as:

$$\frac{\partial^2 \varphi_\Lambda(t)}{\partial t^2} = \frac{i^2 2^{it} \Gamma(L + it)}{\Gamma(L)} \left( [\ln 2 + \psi^0(L + it)]^2 + \psi^1(L + it) \right) \quad (\text{A.8})$$

due to:

$$\begin{aligned}\frac{d2^{it}\Gamma(L+it)}{dt} &= i2^{it}\Gamma(L+it) [\ln 2 + \psi^0(L+it)], \\ \frac{d\psi^0(t)}{dt} &= \psi^1(t), \\ \frac{d\psi^0(L+it)}{dt} &= i\psi^1(L+it), \\ \partial(u \cdot v)/\partial t &= u \cdot \partial v/\partial t + v \cdot \partial u/\partial t,\end{aligned}$$

with  $\psi^1()$  denotes the tri-gamma function.

The  $n^{th}$  moments of random variable  $X$  can be computed from the derivatives of its characteristic function as:

$$E(\Lambda^n) = i^{-n} \varphi_{\Lambda}^{(n)}(0) = i^{-n} \left[ \frac{d^n}{dt^n} \varphi_{\Lambda}(t) \right]_{t=0} \quad (\text{A.9})$$

Thus

$$\begin{aligned}E(\Lambda) &= i^{-1} \left[ \frac{d\varphi_{\Lambda}(t)}{dt} \right]_{t=0} \\ &= i^{-1} \left[ \frac{i2^{it}\Gamma(L+it)}{\Gamma(L)} [\ln 2 + \psi^0(L+it)] \right]_{t=0}\end{aligned}$$

That gives the result:

$$avg(\Lambda) = \psi^0(L) + \ln(2) \quad (\text{A.10})$$

Similarly, for the second moment,

$$\begin{aligned}E(\Lambda^2) &= i^{-2} \left[ \frac{d^2\varphi_{\Lambda}(t)}{dt^2} \right]_{t=0} \\ &= \left[ \frac{2^{it}\Gamma(L+it)}{\Gamma(L)} \left( [\ln 2 + \psi^0(L+it)]^2 + \psi^1(L+it) \right) \right]_{t=0}\end{aligned}$$

That is equivalent to saying that

$$E(\Lambda^2) = [\psi^0(L) + \ln(2)]^2 + \psi^1(L) \quad (\text{A.11})$$

Thus we can state that

$$var(\Lambda) = E(\Lambda^2) - E^2(\Lambda) = \psi^1(L) \quad (\text{A.12})$$

### B. Averages and Variances of POLSAR Covariance Matrix Determinant and Log-Determinant

In this section, the expected value and variance value of these mixture of random variables are derived

$$\chi_L^d \sim \prod_{i=0}^{d-1} \chi(2L - 2i) \quad (\text{A.13})$$

$$\Lambda_L^d \sim \sum_{i=0}^{d-1} \Lambda(2L - 2i) \quad (\text{A.14})$$

given the averages and variances of individual components.

$$\text{avg} [\chi(2L)] = 2L \quad (\text{A.15})$$

$$\text{var} [\chi(2L)] = 4L \quad (\text{A.16})$$

$$\text{avg} [\Lambda(2L)] = \psi^0(L) + \ln 2 \quad (\text{A.17})$$

$$\text{var} [\Lambda(2L)] = \psi^1(L) \quad (\text{A.18})$$

Making use of the mutual independence property of each component  $X_i$ , the variance and expectation of the summation and product of random variables can be written as:

$$\begin{aligned} \text{avg} \left( \sum_{i=1}^n X_i \right) &= \sum_{i=1}^n \text{avg}(X_i), \\ \text{var} \left( \sum_{i=1}^n X_i \right) &= \sum_{i=1}^n \text{var}(X_i), \\ \text{avg} \left( \prod_{i=1}^n X_i \right) &= \prod_{i=1}^n \text{avg}(X_i), \\ \text{var} \left( \prod_{i=1}^n X_i \right) &= \prod_{i=1}^n [\text{avg}^2(X_i) + \text{var}(X_i)] - \prod_{i=1}^n \text{avg}^2(X_i). \end{aligned}$$

Thus they can be rewritten more usefully as:

$$\begin{aligned}
 avg [\chi_L^d] &= 2^d \cdot \prod_{i=0}^{d-1} (L - i), \\
 var [\chi_L^d] &= \prod_{i=0}^{d-1} 4(L - i)(L - i + 1) - \prod_{i=0}^{d-1} 4(L - i)^2, \\
 avg [\Lambda_L^d] &= d \cdot \ln 2 + \sum_{i=0}^{d-1} \psi^0(L - i), \\
 var [\Lambda_L^d] &= \sum_{i=0}^{d-1} \psi^1(L - i)
 \end{aligned}$$

## APPENDIX B

### DERIVING THE CHARACTERISTIC FUNCTIONS FOR THE CONSISTENT MEASURES OF DISTANCE

Given that the characteristic function (CF) of the elementary log-chi square distributions can be written as

$$CF_{\Lambda(2L)}(t) = 2^{it} \Gamma(L + it) / \Gamma(L)$$

then the CF for the following random variables, which are combinations of the above elementary random variables, can be derived

$$\begin{aligned}
 \Lambda_L^d &\sim \sum_{i=0}^{d-1} \Lambda(2L - 2i) \\
 \mathbb{L} &\sim \Lambda_L^d - d \cdot \ln(2L) \\
 \mathbb{D} &\sim \mathbb{L} - d \cdot \ln L + \sum_{i=0}^{d-1} \psi^0(L - i) \\
 \mathbb{C} &\sim \sum_{i=0}^{d-1} [\Lambda(2L - 2i) - \Lambda(2L - 2i)]
 \end{aligned}$$

Since we can state that

$$\begin{aligned}
 CF_{\sum X_i}(t) &= \prod CF_{X_i}(t) \\
 CF_{x+k}(t) &= e^{itk} CF_x(t)
 \end{aligned}$$

then we have:

$$CF_{\Lambda_L^d}(t) = \frac{2^{idt}}{\Gamma(L)^d} \prod_{j=0}^{d-1} \Gamma(L - j + it) \quad (\text{B.19})$$

$$CF_{\mathbb{L}} = \frac{1}{L^{idt} \Gamma(L)^d} \prod_{j=0}^{d-1} \Gamma(L - j + it) \quad (\text{B.20})$$

$$CF_{\mathbb{D}} = \frac{1}{\Gamma(L)^d} \prod_{j=0}^{d-1} e^{idt\psi^0(L-j)} \Gamma(L - j + it) \quad (\text{B.21})$$

Also due to

$$\begin{aligned} CF_{-\Lambda(2L)}(t) &= 2^{-it} \frac{\Gamma(L - it)}{\Gamma(L)} \\ \Delta(2L) &\sim \Lambda(2L) - \Lambda(2L) \\ \Gamma(L - it)\Gamma(L + it) &= \Gamma(2L)B(L - it, L + it) \\ CF_{\Delta(2L)}(t) &= \frac{\Gamma(2L)B(L - it, L + it)}{\Gamma^2(L)} \end{aligned}$$

then we arrive at:

$$CF_{\mathbb{C}} = \prod_{j=0}^{d-1} \frac{\Gamma(2L - 2j)B(L - j - it, L - j + it)}{\Gamma^2(L - j)} \quad (\text{B.22})$$

with  $\Gamma()$  and  $B()$  denoting Gamma and Beta functions respectively.

## APPENDIX C

### SAR INTENSITY AS A SPECIAL CASE OF POLSAR COVARIANCE MATRIX DETERMINANT

In this appendix, the following results for SAR intensity  $I$  are shown to be special cases of the results given in this paper for the determinant of the POLSAR covariance matrix  $\det|C_v|$ . Specifically, the following results extend from the authors previous work on single-look SAR

[20], i.e.  $d = L = 1$ , which is considered a special case. We can state the following:

$$I \sim \bar{I} \cdot pdf[e^{-R}] \quad (C.23)$$

$$\log_2 I \sim \log_2 \bar{I} + pdf[2^{D-2^D}] \quad (C.24)$$

$$\frac{I}{\bar{I}} = \mathbb{R} \sim pdf[e^{-R}] \quad (C.25)$$

$$\log_2 I - \log_2 \bar{I} = \mathbb{D} \sim pdf[2^D e^{-2^D} \ln 2] \quad (C.26)$$

$$\log_2 I_1 - \log_2 I_2 = \mathbb{C} \sim pdf\left[\frac{2^c}{(1+2^c)^2} \ln 2\right] \quad (C.27)$$

$$avg(\mathbb{D}) = -\gamma / \ln 2 \quad (C.28)$$

$$var(\mathbb{D}) = \frac{\pi^2}{6} \frac{1}{\ln^2 2} \quad (C.29)$$

$$mse(\mathbb{D}) = \frac{1}{\ln^2 2} (\gamma^2 + \pi^2/6) = 4.1161 \quad (C.30)$$

but also the following well-known results are considered for multi-look SAR, i.e.  $d = 1, L > 1$ :

$$I \sim pdf\left[\frac{L^L I^{L-1} e^{-LI/\bar{I}}}{\Gamma(L) \bar{I}^L}\right] \quad (C.31)$$

$$N = \ln I \sim pdf\left[\frac{L^L}{\Gamma(L)} e^{L(N-\bar{N}) - Le^{N-\bar{N}}}\right] \quad (C.32)$$

It will be shown that all of these results are special cases of the result derived previously and rewritten below:

$$|C_v| \sim \frac{|\Sigma_v|}{(2L)^d} \prod_{i=0}^{d-1} \chi^2(2L - 2i) \quad (C.33)$$

$$\ln |C_v| \sim \ln |\Sigma_v| + \sum_{i=0}^{d-1} \Lambda(2L - 2i) - d \cdot \ln 2L \quad (C.34)$$

$$\frac{|C_v|}{|\Sigma_v|} = \mathbb{R} \sim \frac{1}{(2L)^d} \prod_{i=0}^{d-1} \chi^2(2L - 2i) \quad (C.35)$$

$$\ln |C_v| - \ln |\Sigma_v| = \mathbb{D} \sim \sum_{i=0}^{d-1} \Lambda(2L - 2i) - d \cdot \ln 2L \quad (C.36)$$

$$\ln |C_{1v}| - \ln |C_{2v}| = \mathbb{C} \sim \sum_{i=0}^{d-1} \Delta(2L - 2i) \quad (C.37)$$

$$avg(\mathbb{D}) = \sum_{i=0}^{d-1} \psi^0(L-i) - d \cdot \ln L \quad (\text{C.38})$$

$$var(\mathbb{D}) = \sum_{i=0}^{d-1} \psi^1(L-i) \quad (\text{C.39})$$

$$mse(\mathbb{D}) = \left[ \sum_{i=0}^{d-1} \psi^0(L-i) - d \cdot \ln L \right]^2 + \sum_{i=0}^{d-1} \psi^1(L-i) \quad (\text{C.40})$$

This appendix also derives new results for multi-look SAR data, which can be thought of either as extensions of the corresponding single-look SAR results or as simple cases of the POLSAR results presented above. They are:

$$\frac{I}{\bar{I}} = \mathbb{R} \sim \frac{1}{2L} \chi^2(2L) \quad (\text{C.41})$$

$$\ln I - \ln \bar{I} = \mathbb{D} \sim \Lambda(2L) - \ln 2L \quad (\text{C.42})$$

$$\ln I_1 - \ln I_2 = \mathbb{C} \sim \Delta(2L) \quad (\text{C.43})$$

$$avg(\mathbb{D}) = \psi^0(L) - \ln L \quad (\text{C.44})$$

$$var(\mathbb{D}) = \psi^1(L) \quad (\text{C.45})$$

$$mse(\mathbb{D}) = [\psi^0(L) - \ln L]^2 + \psi^1(L) \quad (\text{C.46})$$

The derivation process detailed below consists of two-phases. The first phase collapses the generic multi-dimensional POLSAR results into the classical one-dimensional SAR domain. Mathematically this means setting the dimensional number in POLSAR to  $d = 1$  and collapsing the POLSAR covariance matrix into the variance measure in SAR, which also equals the SAR intensity i.e.  $|C_v| = I, |\Sigma_v| = \bar{I}$ .

The output of the first phase, in the general case, is applicable to multi-look SAR data, where  $d = 1$  but  $L > 1$ . The second phase simplifies the multi-look results into single-look results, which will match those presented in our previous work [20]. Mathematically, it means setting  $L = 1$  in the multi-look result and converting from the natural logarithmic domain used in this paper to the base-2 logarithm used in [20] (base-2 was chosen in the previous paper to simplify the computation).



### A. Original Domain: SAR Intensity and its ratio

Setting  $d = 1$ ,  $|C_v| = I$  and  $|\Sigma_v| = \bar{I}$  into Eqns. C.33 and C.35 we find that:

$$I \sim \frac{\bar{I}}{2L} \chi^2(2L)$$

$$\frac{I}{\bar{I}} = \mathbb{R} \sim \frac{1}{2L} \chi^2(2L)$$

Or in PDF forms, and applying the variable change theorem,:

$$\begin{aligned} \frac{2LI}{\bar{I}} &\sim \text{pdf} \left[ \frac{x^{L-1} e^{-x/2}}{2^L \Gamma(L)} \right] \\ \frac{I}{\bar{I}} &\sim \text{pdf} \left[ \frac{x^{L-1} e^{-x/2}}{2^L \Gamma(L)} \cdot dx/dt \right]_{x=2L \cdot t} \\ &\sim \text{pdf} \left[ \frac{L^L t^{L-1} e^{-Lt}}{\Gamma(L)} \right] \\ I &\sim \text{pdf} \left[ \frac{L^L t^{L-1} e^{-Lt}}{\Gamma(L)} \cdot dt/dx \right]_{t=x/\bar{I}} \\ &\sim \text{pdf} \left[ \frac{L^L x^{L-1} e^{-Lx/\bar{I}}}{\bar{I}^L \Gamma(L)} \right] \end{aligned}$$

Thus we have the following results for multi-look SAR:

$$I \sim \text{pdf} \left[ \frac{L^L x^{L-1} e^{-Lx/\bar{I}}}{\bar{I}^L \Gamma(L)} \right] \quad (\text{C.47})$$

$$\frac{I}{\bar{I}} = \mathbb{R} \sim \text{pdf} \left[ \frac{L^L x^{L-1} e^{-Lx}}{\Gamma(L)} \right] \quad (\text{C.48})$$

Now setting  $L = 1$ , these results become:

$$I \sim \text{pdf} \left[ \frac{e^{x/\bar{I}}}{\bar{I}} \right] \quad (\text{C.49})$$

$$\frac{I}{\bar{I}} = \mathbb{R} \sim \text{pdf} [e^{-x}] \quad (\text{C.50})$$

which is the same as stated in [20], demonstrating that the previous work is a special case of the more generic POLSAR forms.

### B. Log-transformed domain: SAR log-intensity and the log-distance

The result for multi-look SAR data written in the log-transformed domain can be derived from two different approaches. The first is to follow a simplification method, where the results for log-transformed POLSAR data are simplified into log-transformed multi-look SAR results.

The second approach is to apply log-transformation to the results derived in the previous section. In this section, it is shown that both approaches would result in identical results.

Setting  $d = 1$ ,  $|C_v| = I$  and  $|\Sigma_v| = \bar{I}$  into Eqns. C.34 and C.36 we have

$$\begin{aligned}\ln I &\sim \ln \bar{I} + \Lambda(2L) - \ln 2L \\ \ln I - \ln \bar{I} = \mathbb{L} &\sim \Lambda(2L) - \ln 2L\end{aligned}$$

Or in PDF form, and applying the variable change theorem we have:

$$\begin{aligned}\ln I - \ln \bar{I} + \ln 2L &\sim \text{pdf} \left[ \frac{e^{Lx - e^x/2}}{2^L \Gamma(L)} \right] \\ \ln I - \ln \bar{I} &\sim \text{pdf} \left[ \frac{e^{Lx - e^x/2}}{2^L \Gamma(L)} \cdot dx/dt \right]_{x=t+\ln 2L} \\ &\sim \text{pdf} \left[ \frac{L^L e^{Lt - Le^t}}{\Gamma(L)} \right] \\ \ln I &\sim \text{pdf} \left[ \frac{L^L e^{Lt - Le^t}}{\Gamma(L)} \cdot dt/dx \right]_{t=x-\ln \bar{I}} \\ &\sim \text{pdf} \left[ \frac{L^L e^{L(x-\bar{N}) - Le^{x-\bar{N}}}}{\Gamma(L)} \right]\end{aligned}$$

with  $\bar{N} = \ln \bar{I}$ . Thus the first approach arrives at

$$\ln I = \mathbb{N} \sim \text{pdf} \left[ \frac{L^L e^{L(x-\bar{N}) - Le^{x-\bar{N}}}}{\Gamma(L)} \right] \quad (\text{C.51})$$

$$\ln I - \ln \bar{I} = \mathbb{L} \sim \text{pdf} \left[ \frac{L^L e^{Lt - Le^t}}{\Gamma(L)} \right] \quad (\text{C.52})$$

In the second approach, log-transformation is applied on previous results for multi-look SAR intensity and its ratio in the original domain (Eqns. C.48 and C.47). This also arrives at the same results shown above, however the detailed working is omitted for brevity.

To compute summary statistics for the multi-look SAR dispersion, set  $d = 1$  into Eqns. C.40, C.38 and C.39 we have:

$$\begin{aligned}\text{avg}(\mathbb{L}) &= \psi^0(L) - \ln L \\ \text{var}(\mathbb{L}) &= \psi^1(L) \\ \text{mse}(\mathbb{L}) &= [\psi^0(L) - \ln L]^2 + \psi^1(L)\end{aligned}$$

This completes the first phase of the derivation process. The second phase of simplification involves setting  $L = 1$  into the above results for multi-look SAR data, and converting natural logarithm into base-2 logarithm. First, setting  $L = 1$  makes the above results become

$$\begin{aligned}\ln I = \mathbb{N} &\sim pdf \left[ e^{(x-\bar{N})-e^{x-\bar{N}}} \right] \\ \ln I - \ln \bar{I} = \mathbb{L} &\sim pdf \left[ e^{x-e^x} \right] \\ avg(\mathbb{L}) &= \psi^0(1) = -\gamma \\ var(\mathbb{L}) &= \psi^1(1) = \pi^2/6 \\ mse(\mathbb{L}) &= [\psi^0(1)]^2 + \psi^1(1) = \gamma^2 + \pi^2/6\end{aligned}$$

with  $\gamma$  denoting the Euler-Mascharoni constant. Then to convert to base-2 logarithm from natural logarithmic transformation, we again use the variable change theorem. That is:

$$\begin{aligned}\log_2 I = \mathbb{N}_2 &\sim pdf \left[ e^{(x-\bar{N})-e^{x-\bar{N}}} \cdot dx/dt \right]_{x=t \cdot \ln 2} \\ \mathbb{N}/\ln 2 = \mathbb{N}_2 &\sim pdf \left[ e^{(t \cdot \ln 2 - \bar{N}) - e^{t \cdot \ln 2 - \bar{N}}} \ln 2 \right]_{\bar{N}_2 = \bar{N} \cdot \ln 2} \\ &\sim pdf \left[ 2^{t-\bar{N}_2} e^{2^t - \bar{N}_2} \ln 2 \right] \\ \log_2 I - \log_2 \bar{I} = \mathbb{L}/\ln 2 = \mathbb{L}_2 &\sim pdf \left[ e^{x-e^x} \right]_{x=t \cdot \ln 2} \\ &\sim pdf \left[ 2^t e^{2^t} \ln 2 \right] \\ avg(\mathbb{L}_2) &= avg(\mathbb{L})/\ln 2 = -\gamma/\ln 2 \\ var(\mathbb{L}_2) &= var(\mathbb{L})/\ln^2 2 = \frac{\pi^2}{6} \frac{1}{\ln^2 2} \\ mse(\mathbb{L}_2) &= mse(\mathbb{L})/\ln^2 2 = \frac{1}{\ln^2 2} (\gamma^2 + \pi^2/6) = 4.1161\end{aligned}$$

### C. Deriving the PDF for SAR dispersion and contrast

The PDF for SAR dispersion can be easily derived from the PDF for the log-distance given above as:

$$\ln I - avg(\ln I) = \mathbb{D} \sim pdf \left[ \frac{e^{L[x+\psi^0(L)] - Le^{x+\psi^0(L)-\ln L}}}{\Gamma(L)} \right] \quad (\text{C.53})$$

due to  $d = 1$  and

$$\begin{aligned}\mathbb{D} &\sim \mathbb{L} - \text{avg}(\mathbb{L}) \\ \text{avg}(\mathbb{L}) &= \psi^0(L) - \ln L \\ \mathbb{L} &\sim \text{pdf} \left[ \frac{L^L e^{Lt - Le^t}}{\Gamma(L)} \right]\end{aligned}$$

Setting  $L = 1$  for Single-Look SAR we have

$$\mathbb{D} \sim \text{pdf} \left[ e^{x - \gamma - e^{x - \gamma}} \right] \quad (\text{C.54})$$

due to:  $\psi^0(1) = -\gamma$  and  $\Gamma(1) = 1$  with  $\gamma$  being the Euler Mascheroni constant (which equals 0.5772). In base-2 logarithm domain, invoking the variable change theorem:

$$\begin{aligned}\mathbb{D}_2 &= \log_2 I - \text{avg}(\log_2 I) = \mathbb{D} / \ln 2 \\ \mathbb{D}_2 &\sim \text{pdf} \left[ e^{x - \gamma - e^{x - \gamma}} \cdot \frac{dx}{dt} \right]_{x=t \cdot \ln 2}\end{aligned}$$

Thus we have

$$\mathbb{D}_2 \sim \text{pdf} \left[ e^{-(2^x e^{-\gamma})} (2^x e^{-\gamma}) \ln 2 \right] \quad (\text{C.55})$$

which is consistent with the results found in our previous work [20].

Setting  $d = 1$  into Eqn. for contrast results in

$$\ln I_1 - \ln I_2 = \mathbb{C} \sim \Delta(2L) \quad (\text{C.56})$$

The characteristic function would then be

$$CF_{\mathbb{C}} = \frac{\Gamma(2L) B(L - it, L + it)}{\Gamma(L)^2} \quad (\text{C.57})$$

Thus the PDF can be written as

$$\mathbb{C} \sim \text{pdf} \left[ \frac{\Gamma(2L)}{\Gamma(L)^2} \frac{e^{Lx}}{(1 + e^x)^{2L}} \right] \quad (\text{C.58})$$

due to

$$\begin{aligned}CF_{\mathbb{C}}(x) &= \frac{\Gamma(2L)}{\Gamma(L)^2} B(1/(1 + e^x), L - it, L + it) \\ &= \frac{\Gamma(2L)}{\Gamma(L)^2} \int_0^{1/(1 + e^x)} z^{L - it - 1} (1 - z)^{L + it - 1} dz \\ \frac{\partial}{\partial x} CF_{\mathbb{C}}(x) &= \frac{\partial CF_{\mathbb{C}}(x)}{\partial 1/(1 + e^x)} \cdot \frac{\partial 1/(1 + e^x)}{\partial x} \\ &= e^{itx} \frac{\Gamma(2L)}{\Gamma(L)^2} \frac{e^{Lx}}{(1 + e^x)^{2L}}\end{aligned}$$

Setting  $L = 1$  into Eqn. C.58 we have the PDF for contrast of single-look SAR data:

$$\mathbb{C} \sim pdf \left[ \frac{e^x}{(1 + e^x)^2} \right] \quad (\text{C.59})$$

Converting to base-2 logarithm gives the following:

$$\begin{aligned} \mathbb{C}/\ln 2 = \mathbb{C}_2 &\sim pdf \left[ \frac{e^x}{(1 + e^x)^2} \cdot dx/dt \right]_{x=t \cdot \ln 2} \\ &\sim pdf \left[ \ln 2 \frac{2^t}{(1 + 2^t)^2} \right] \end{aligned}$$

which is also consistent to the results shown in our previous work [20].

## REFERENCES

- [1] K. Conradsen, A. Nielsen, J. Schou, and H. Skriver, "A test statistic in the complex Wishart distribution and its application to change detection in polarimetric SAR data," *IEEE Transactions on Geoscience and Remote Sensing*, vol. 41, no. 1, pp. 4 – 19, Jan 2003.
- [2] M. Dabboor, J. Yackel, M. Hossain, and A. Braun, "Comparing matrix distance measures for unsupervised POLSAR data classification of sea ice based on agglomerative clustering," *International Journal of Remote Sensing*, vol. 34, no. 4, pp. 1492–1505, 2013.
- [3] P. Kersten, J. S. Lee, and T. Ainsworth, "Unsupervised classification of polarimetric synthetic aperture radar images using fuzzy clustering and EM clustering," *IEEE Transactions on Geoscience and Remote Sensing*, vol. 43, no. 3, pp. 519 – 527, Mar 2005.
- [4] J.-S. Lee, M. Grunes, and G. de Grandi, "Polarimetric SAR speckle filtering and its implication for classification," *IEEE Transactions on Geoscience and Remote Sensing*, vol. 37, no. 5, pp. 2363 –2373, Sep 1999.
- [5] J. S. Lee, M. R. Grunes, and R. Kwok, "Classification of multi-look polarimetric SAR imagery based on complex Wishart distribution," *International Journal of Remote Sensing*, vol. 15, no. 11, pp. 2299–2311, 1994.
- [6] S. N. Anfinsen, R. Jenssen, and T. Eltoft, "Spectral clustering of polarimetric SAR data with Wishart-derived distance measures," in *3rd International Workshop on Science and Applications of SAR Polarimetry and Polarimetric Interferometry*, vol. 3, Jan 2007.
- [7] K. Y. Lee and T. Bretschneider, "Derivation of separability measures based on central complex Gaussian and Wishart distributions," in *IEEE International Geoscience and Remote Sensing Symposium (IGARSS), 2011*, Jul 2011, pp. 3740 –3743.
- [8] F. Cao, W. Hong, Y. Wu, and E. Pottier, "An unsupervised segmentation with an adaptive number of clusters using the SPAN/H/ $\alpha$ /A space and the complex Wishart clustering for fully polarimetric SAR data analysis," *IEEE Transactions on Geoscience and Remote Sensing*, vol. 45, no. 11, pp. 3454 –3467, Nov 2007.
- [9] V. Alberga, G. Satalino, and D. K. Staykova, "Comparison of polarimetric sar observables in terms of classification performance," *International Journal of Remote Sensing*, vol. 29, no. 14, pp. 4129–4150, 2008. [Online]. Available: <http://www.tandfonline.com/doi/abs/10.1080/01431160701840182>
- [10] R. Barakat, "The statistical properties of partially polarized light," *Optica Acta: International Journal of Optics*, vol. 32, no. 3, pp. 295–312, 1985. [Online]. Available: <http://www.tandfonline.com/doi/abs/10.1080/713821736>

- [11] D. Eliyahu, "Vector statistics of correlated gaussian fields," *Phys. Rev. E*, vol. 47, pp. 2881–2892, Apr 1993. [Online]. Available: <http://link.aps.org/doi/10.1103/PhysRevE.47.2881>
- [12] C. Brosseau, "Statistics of the normalized stokes parameters for a gaussian stochastic plane wave field," *Appl. Opt.*, vol. 34, no. 22, pp. 4788–4793, Aug 1995. [Online]. Available: <http://ao.osa.org/abstract.cfm?URI=ao-34-22-4788>
- [13] I. Joughin, D. Winebrenner, and D. Percival, "Probability density functions for multilook polarimetric signatures," *Geoscience and Remote Sensing, IEEE Transactions on*, vol. 32, no. 3, pp. 562–574, may 1994.
- [14] J.-S. Lee, K. Hoppel, S. Mango, and A. Miller, "Intensity and phase statistics of multilook polarimetric and interferometric SAR imagery," *IEEE Transactions on Geoscience and Remote Sensing*, vol. 32, no. 5, pp. 1017–1028, Sep 1994.
- [15] R. Touzi and A. Lopes, "Statistics of the stokes parameters and of the complex coherence parameters in one-look and multilook speckle fields," *Geoscience and Remote Sensing, IEEE Transactions on*, vol. 34, no. 2, pp. 519–531, mar 1996.
- [16] C. Lopez-Martinez and X. Fabregas, "Polarimetric sar speckle noise model," *Geoscience and Remote Sensing, IEEE Transactions on*, vol. 41, no. 10, pp. 2232–2242, 2003.
- [17] E. Erten, "The performance analysis based on SAR sample covariance matrix," *Sensors (Basel)*, vol. 12, no. 3, pp. 2766–2786, 2012.
- [18] N. R. Goodman, "The distribution of the determinant of a complex Wishart distributed matrix," *Annals of Mathematical Statistics*, vol. 34, no. 1, pp. 178–180, 1963.
- [19] T. H. Le, I. V. McLoughlin, K. Y. Lee, and T. Brestchneider, "SLC SAR speckle filtering using homoskedastic features of logarithmic transformation," in *Proceedings of the 31th Asian Conference on Remote Sensing (ACRS)*, Hanoi, Vietnam, Nov 2010.
- [20] T. H. Le, I. V. McLoughlin, Q. H. Nguyen, and C. H. Vun, "Using MSE to evaluate SAR speckle filters," *IEEE Transactions on Geoscience and Remote Sensing*, vol. ??, no. ??, pp. ???–???, ??? 2013, (Work-In-Progress).
- [21] R. Raney and G. Wessels, "Spatial considerations in SAR speckle consideration," *IEEE Transactions on Geoscience and Remote Sensing*, vol. 26, no. 5, pp. 666–672, Sep 1988.
- [22] S. Anfinson, A. Doulgeris, and T. Eltoft, "Estimation of the equivalent number of looks in polarimetric synthetic aperture radar imagery," *IEEE Transactions on Geoscience and Remote Sensing*, vol. 47, no. 11, pp. 3795–3809, Nov 2009.
- [23] "AIRSAR implementation," [Accessed Feb 2013]. [Online]. Available: <http://airsar.jpl.nasa.gov/documents/genairsar/chapter3.pdf>
- [24] "RadarSat-2 product description," [Accessed Feb 2013]. [Online]. Available: [http://gs.mdacorporation.com/products/sensor/radarsat2/RS2\\_Product\\_Description.pdf](http://gs.mdacorporation.com/products/sensor/radarsat2/RS2_Product_Description.pdf)
- [25] E. Rignot and J. van Zyl, "Change detection techniques for ERS-1 SAR data," *IEEE Transactions on Geoscience and Remote Sensing*, vol. 31, no. 4, pp. 896–906, Jul 1993.
- [26] F. Medeiros, N. Mascarenhas, and L. Costa, "Evaluation of speckle noise MAP filtering algorithms applied to SAR images," *International Journal of Remote Sensing*, vol. 24, no. 24, pp. 5197–5218, Dec 2003.
- [27] A. Freeman and S. Durden, "A three-component scattering model for polarimetric SAR data," *IEEE Transactions on Geoscience and Remote Sensing*, vol. 36, no. 3, pp. 963–973, May 1998.
- [28] S. Cloude and E. Pottier, "An entropy based classification scheme for land applications of polarimetric SAR," *IEEE Transactions on Geoscience and Remote Sensing*, vol. 35, no. 1, pp. 68–78, Jan 1997.
- [29] J. Schou, H. Skriver, A. Nielsen, and K. Conradsen, "CFAR edge detector for polarimetric SAR images," *IEEE Transactions on Geoscience and Remote Sensing*, vol. 41, no. 1, pp. 20–32, Jan 2003.
- [30] T. H. Le and I. V. McLoughlin, "SAR Fuzzy-MLE speckle filter using the distance consistency property in homoskedastic

log-transformed domain,” in *Proceedings of the 32th Asian Conference on Remote Sensing (ACRS)*, Taipei, Taiwan, Nov 2011.